POLITECNICO
MILANO 1863

SCUOLA DI INGEGNERIA INDUSTRIALE
E DELL'INFORMAZIONE

Extended Weighted Least Squares (EWLS) Estimator Performance Analysis

Tesi di Laurea Magistrale in
Electrical Engineering - Ingegneria Elettrica

Author: **Yiqiao He**

Student ID: 10830231
Supervisor: Prof. Gabriele D'Antona
Academic Year: 2022-23

Abstract

State estimation (SE) is an important method used in the control operations of modern power systems. The SE method relies on an overabundance of data with a power system model which associates the unknown state variables to them. As the set of measurement data is typically characterized by a degree of uncertainty, SE is capable of utilizing its overabundance to further narrow the error caused in the final estimated state. However, the classical weight least squared method takes only the uncertainty present in the data provided by measurement instruments while neglecting the possible impact of uncertain parameters. To address this particular problem, a WLS approach is proposed in [6], specifically the extended WLS (EWLS) approach .

In this thesis, a complex system model with artificially controlled uncertainty is adopted to extensively test the proposed method and a detailed comparison with the classical WLS is provided. With IEEE14 bus system served as an example, a Monte Carlo trial is performed to verify the effectiveness and robustness of aforementioned method. Results are then analyzed both graphically and numerically.

Keywords: state estimation, least squared method, power system monitoring, power system simulation, uncertain systems

Sommario

La stima dello stato (SE) è un metodo importante utilizzato nelle operazioni di controllo dei moderni sistemi di potenza. Il metodo SE si basa su una sovrabbondanza di dati con un modello di sistema elettrico che associa ad essi le variabili di stato sconosciute. Poiché l'insieme dei dati di misura è tipicamente caratterizzato da un certo grado di incertezza, il metodo SE è in grado di utilizzare la sua sovrabbondanza per ridurre ulteriormente l'errore causato dallo stato finale stimato. Tuttavia, il classico metodo dei minimi quadrati ponderati considera solo l'incertezza presente nei dati forniti dagli strumenti di misura, trascurando il possibile impatto dei parametri incerti. Per affrontare questo particolare problema, è stato proposto un nuovo approccio WLS, in particolare l'approccio WLS esteso (EWLS) [6].

In questa tesi, viene adottato un modello di sistema complesso con incertezza controllata artificialmente per testare estensivamente il metodo proposto e viene fornito un confronto dettagliato con il WLS classico. Prendendo come esempio il sistema di bus IEEE14, si esegue una prova Monte Carlo per verificare l'efficacia e la robustezza di questo metodo. I risultati sono analizzati sia graficamente che numericamente.

Keywords: Stima dello stato, metodo dei minimi quadrati, monitoraggio del sistema elettrico, simulazione del sistema elettrico, sistemi incerti

Contents

Introduction

Electric power system control relies heavily on an accurate evaluation of system states to maintain the reliability and continuity of the service. Specifically, the state consists of a set of variables: the voltage magnitude and according phase of each bus, which are necessary for the system operators to dictate security plans, evaluate possible contingencies, and perform various control actions. Therefore, a way to obtain such sets of variable, both quickly and with suitable accuracy, is vital to help keep a modern power system in check.

In the planning phase of a network, a load-flow (LF) study is typically performed. LF method involves computing state variables from active and reactive in-line power flowing, in addition to parameters of the lines, all of which are known through choices made in designation of the system. Thus, state variables obtained this way can be considered perfect for the ideal system in a given condition.

However, the LF approach possesses several problems: Firstly, it requires a complete set of power flow measurements, which may not be available in practice. Moreover, measurements in reality will inevitably contain errors, but LF is incapable of taking those into account. Most importantly, it is not possible for LF method to process additional redundant data in order to reduce the impact of inaccuracy in measurement. Therefore, to evaluate the actual state of a working electric power system, a State Estimation (SE) approach is necessary. [11]

SE is based on a redundant set of data, often characterized by a certain degree of uncertainty, which the method then proceed to address through links between available data and state variables, derived from the given model itself. In this way, the redundancy of the data can be exploited to reduce the impact of its inaccuracy on the computed state.

Typically, the data given to an SE algorithm are either measurements directly from telemeters installed on the network, or pseudo-measurements from prior knowledge. Regarding the power system model, however, generally only the latter are available, as they come from a quasi-static mathematical model of the system, rather than from on-site measuring. Still, uncertainty affects those network parameters also, as in practice there are many issues in a power system that could lead to inaccuracy, such as the geometrical placement

of power lines, temperature deviation due to weather or loading conditions, or even potential unbalance in the system that were overlooked by the mathematical model. In any case, obtained parameters in such way are far from accurate.

In electric power systems, the Weighted Least Squares (WLS) approach is the most well-known technique employed in SE method, first proposed in the early 1970s [16] [11] [9]. This approach gives an uncertain analysis of the measurement data based on a static power system model assumed to be exact (as in perfectly certain).

This assumption, however, while it allows for a simpler approach on the problem, risks a significant bias on the state. As is mentioned before, network parameters are uncertain as well. In fact, often those parameters are even considered less accurate than measurements [2] [17], giving a considerable contribution to the uncertainty of the state. It may be also worth noting that such risks rise further as the accuracy of measurement improves, as the proportion of parameters' contribution will increase.

To address this concern, many effective network parameter estimation (PE) methods are proposed. Some of them rely on a residual sensitivities analysis, while others utilise the normal equation or adopt a Kalman filter [13] [19] [20]. Although those PE methods are capable of improving SE performance, they still do not directly account for the problem of including uncertain parameters in an SE method.

In this thesis, a detailed system model based on MATLAB for a generalization of the classic WLS and then a novel extended WLS method [6], accounting for uncertainty in both measurements and network parameters, is established. Using IEEE14 bus system as an example, a Monte Carlo trial is then performed to verify the effectiveness and robustness of aforementioned methods under various circumstances. Finally, results drawn from different case are extensively studied, along with both graphical analysis as well as numerical tests.

0.1. Thesis overview

Chapter 1: Provides the basic modelling of the system. How transmission lines, shunts, tap-changing transformers and various network components are accounted for in the simulation are explained in this chapter. The classical WLS method for state estimation is also introduced.

Chapter 2: Proposed WLS methods to be tested on, specifically, GWLS and EWLS are introduced. The difference between them, the potential advantages and disadvantages are explained.

Chapter 3: The framework of the simulation is established. A flowchart of the test process is shown and parts of the algorithm are explained in detail.

Chapter 4: Four different cases are tested with the above simulation based on MATLAB. For each case, results are plotted and numerically analyzed. Considerations on the used methods are given.

Chapter 5: A summary of the thesis work is provided, with some discussions about future work included.

1 | Classical Modelling

1.1. System Modelling

In this chapter, the modelling and associated definitions of power systems used in the following discussion and simulation tests are provided. The classical WLS state estimation method is also briefly discussed.

1.1.1. Transmission Lines

Transmission lines are represented by a two-port π-model as shown in figure 1.1 [7]. Parameters of a line correspond to the equivalent circuit of its positive sequence, composed of a series impedance $R + jX$ and the total line charging susceptance $j2B$.

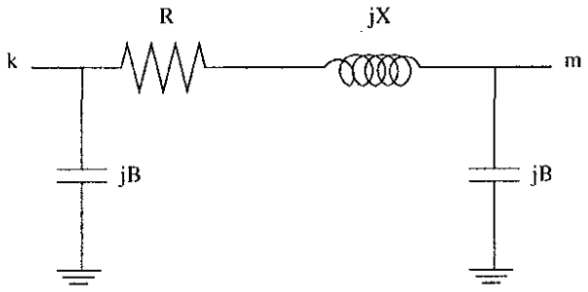

Figure 1.1: Transmission line model [5]

1.1.2. Tap-changing Transformers

Tap-changing transformers are modelled as impedance in series with ideal transformers as shown in figure 1.2. [5]

The nodal equation of the 2-port circuit excluding the tap-changer transformer [5] is:

$$\begin{bmatrix} \overline{I}_p \\ \overline{I}_k \end{bmatrix} = \begin{bmatrix} y & -y \\ -y & y \end{bmatrix} \begin{bmatrix} \overline{V}_p \\ \overline{V}_k \end{bmatrix} \tag{1.1}$$

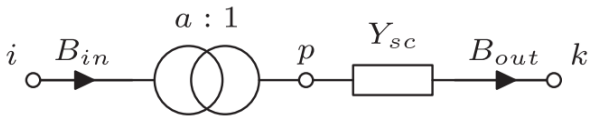

Figure 1.2: Tap-changing transformer in a transmission line model [5]

in which:

$$\begin{aligned} \overline{I}_p &= a \cdot \overline{I}_i \\ \overline{V}_p &= \overline{V}_i / a \end{aligned} \tag{1.2}$$

where a is the tap ratio.

Thus obtaining:

$$\begin{bmatrix} \overline{I}_p \\ \overline{I}_k \end{bmatrix} = \begin{bmatrix} y/a^2 & -y/a \\ -y/a & y \end{bmatrix} \begin{bmatrix} \overline{V}_p \\ \overline{V}_k \end{bmatrix} \tag{1.3}$$

Rearranging the form to adapt the π-model introduced in the beginning of the chapter, the following can be obtained:

$$\begin{aligned} \overline{Y}_{ik} &= \frac{y}{a} \\ \overline{Y}_i &= \frac{1-a}{a^2} y \\ \overline{Y}_k &= \frac{a-1}{a} y \end{aligned} \tag{1.4}$$

Therefore, the equivalent transformer π-model would be:

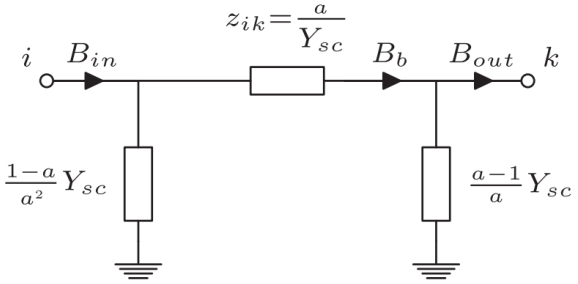

Figure 1.3: π-model of the Tap-changing Transformer

1.2. State and Measurement Formulation

In this section, the notation conventions used in the following pages will be introduced.

1.2.1. Network Parameters and Topology

A P-vector π contains the values of various network parameters (resistance, reactance, charging susceptance, transformer tap ratio and other potential factors regarding certain properties of the network), while a K-vector k represents the topology of the network:

$$\pi \in \mathbf{R}^{M\times 1}, k \in \mathbf{Z}^{K\times 1} \tag{1.5}$$

1.2.2. State

An N-vector x contains the static-state of the system.

$$x \in \mathbf{R}^{N\times 1} \tag{1.6}$$

For a power system with a bus number of n,

$$N = 2n - 1 \tag{1.7}$$

which corresponds to the voltage magnitude and phase of each bus (minus the slack for phases).

1.2.3. Measurement Data

The measurement and pseudo-measurement data are stored in a M-vector y, which is related to the state by the following relationship expressing the power system model:

$$y = f(x_t; \pi_t, k_t) \in \mathbf{R}^{M\times 1} \tag{1.8}$$

in which the subscript t represents true value.

However, since measurements, pseudo-measurements, network parameters and topology are all affected by some degrees of uncertainty, in general it is not possible to find a general solution x:

$$y \neq f(x_t; \pi, k) \tag{1.9}$$

with

$$\begin{aligned} y &= y_t + \Delta y \\ \pi &= \pi_t + \Delta\pi, k = k_t + \Delta k \end{aligned} \tag{1.10}$$

in which $\Delta y, \Delta\pi, \Delta k$ are respective errors incurred in the modelling or measuring.

Therefore, in a real power system the following equation must be used:

$$y - \Delta y = f(x_t; \pi - \Delta\pi, k - \Delta k) \tag{1.11}$$

For the sake of simplicity, information about network topology is considered perfect in this thesis. Thus, the vector k will be dropped from the arguments:

$$y - \Delta y = f(x_t; \pi - \Delta\pi) \tag{1.12}$$

Performing a Taylor Series expansion of 1.12 with respect to vector π yields:

$$y - \Delta y \approx f(x_t; \pi) - \left.\frac{\partial f}{\partial \pi^T}\right|_{x_t,\pi} \cdot \Delta\pi \tag{1.13}$$

In order to reach a more compact form, the vector d is introduced:

$$d = \begin{bmatrix} y \\ \pi \end{bmatrix} \in \mathbf{R}^{(M+P)\times 1} \tag{1.14}$$

refining 1.13:

$$r(x_t; d) \approx A(x_t; \pi) \cdot \Delta d \tag{1.15}$$

in which r is the misfit:

$$r(x_t; d) = y - f(x_t; \pi) \tag{1.16}$$

Δd is the error of data:

$$\Delta d = \begin{bmatrix} \Delta y \\ \Delta \pi \end{bmatrix} \tag{1.17}$$

and A is the matrix:

$$A(x_t; \pi) = [I_M \quad -\frac{\partial f}{\partial \pi^T}] \in \mathbf{R}^{M \times (M+P)} \tag{1.18}$$

1.3. Weighted Least Square (WLS) Approach

In the classical WLS approach, the assumption that only measurements y are affected by errors is made, while the uncertainty of parameters π is ignored. Therefore, the data error is:

$$\Delta d = \begin{bmatrix} \Delta y \\ 0_P \times 1 \end{bmatrix} \tag{1.19}$$

Consequently, only the measurement errors have an impact on the misfit:

$$r(x_t; d) = \Delta y \tag{1.20}$$

From here, as long as we have enough measurement data to ensure $M > N$, the state estimation can be defined as an overdetermined problem and may be formalized in the following way:

$$\begin{aligned} &\underset{x, \Delta y}{argmin} |\Delta y|^2_{\Sigma y} \\ &s.t. \Delta y = y - f(x; \pi) \end{aligned} \tag{1.21}$$

where Σ_y is the variance-covariance matrix of the random measurement errors, signalling the uncertainty of the measurements. The norm weighted by the covariance matrix in 1.21 is then expressed as:

$$|\Delta y|^2_{\Sigma y} = r^T \cdot \Sigma_y^{-1} \cdot r \tag{1.22}$$

Now, to solve the minimum problem, Newton-Gauss method can be applied to form an

iterative solution:

$$\Delta\tilde{x}_k = G^{-1}_{\tilde{x}_k} \, (\frac{\partial f}{\partial \tilde{x^T}})_{\tilde{x}_k,\pi} \, \Sigma_y^{-1} \, \tilde{r} \tag{1.23}$$

where $G^{-1}_{\tilde{x}_k}$ is the gain matrix:

$$G_{\tilde{x}_k} = (\frac{\partial f}{\partial \tilde{x}^T})^T_{\tilde{x}_k,\pi} \, \Sigma_y^{-1} \, (\frac{\partial f}{\partial \tilde{x}^T})_{\tilde{x}_k,\pi} \tag{1.24}$$

The algorithm can then perform the state estimation by iterating $\tilde{x_k}$:

$$\tilde{x}_{k+1} = \tilde{x}_k + \Delta\tilde{x_k} \tag{1.25}$$

2 | Proposed WLS Methods

The WLS approach treats parameters to be certain in its evaluation of the state. However, this is far from true and could lead to vast underestimation of the errors presented in the final calculated state.

In reality, many factors affect the working parameter of an electric network, especially when concerning the transmission lines [18] [1]. Despite often treated by the system operators according to a constant, pre-defined value, the real properties of a line, in addition to its length, type of conductor material, may also be affected by:

- Actual geometry of the line;
- Weather, in which the change of temperature can lead to vast variation of line resistance;
- Loading conditions, which can lead to overheating of the lines.

In this chapter, two novel WLS methods proposed in [6] and this thesis meant to test on will be introduced.

Firstly a generalization of the classical WLS (GWLS) method will be presented. This method considers the effect of parameter errors as an addition to the existing WLS method, addressing the problem without changing too much of the original structure. However this method lacks the ability to distinguish the source of uncertainty contribution due to the same simplification.

Then, on the basis of GWLS, a further enhanced extended WLS method which this thesis mainly focuses on is also shown. This method, on the other hand, takes a more straightforward approach, taking uncertainty on measurements and parameters in its computation. With EWLS it is possible to do further bad data analysis on the results. In addition, EWLS also has a higher endurance to bad initial state than GWLS does.

2.1. Generalized WLS

In this generalization of the old WLS approach (GWLS), the uncertainty of the network parameters is dealt with by considering it an artificial error set upon the already existing measurement errors $\Delta\tilde{y}$.

$$\Delta y' = y - f(x,\pi) \approx \Delta y - \left.\frac{\partial f}{\partial \pi^T}\right|_{x_t,\pi} \cdot \Delta\pi \tag{2.1}$$

However, since in practice the true state $\tilde{x}_t$ is unknown, 2.1 should be rewritten as:

$$\Delta y' \approx \Delta y - \left.\frac{\partial f}{\partial \pi^T}\right|_{x_0,\pi} \cdot \Delta\pi - \frac{\partial}{\partial x^T}\left(\frac{\partial f}{\partial \pi^T}\Delta\pi\right)_{x_0,\pi} \cdot \Delta x_0 \tag{2.2}$$

where $\tilde{x}_0$ represents the initial guess of the true state $\tilde{x}_t$.

The added measurement error can then lead to an updated version of the variance-covariance matrix Σ_y:

$$\Sigma'_y \approx \Sigma_y + \left(\frac{\partial f}{\partial \pi^T}\right)_{x0,\pi} \Sigma_\pi \left(\frac{\partial f}{\partial \pi^T}\right)^T_{x0,\pi} + \left(\frac{\partial^2 f}{\partial \pi^T \partial x^T}\right)_{x0,\pi} (\Sigma_{x_0} \otimes \Sigma_\pi) \left(\frac{\partial^2 f}{\partial \pi^T \partial x^T}\right)^T_{x0,\pi} \tag{2.3}$$

The new Σ'_y now takes the errors related to measurements, parameters and the initial state guess into consideration, while also considers them all uncorrelated to each other. In the case where some of them do correlate to others (e.g. some of the network parameter data are derived from on-line measurements), however, Σ'_y needs to be worked upon further by handling the uncertainty propagation properly.

Anyhow, the WLS estimation problem can now be redefined as:

$$\begin{aligned} &\underset{x,\Delta y}{argmin} |\Delta y|^2_{\Sigma y'} \\ &s.t. \Delta y = y - f(x;\pi) \end{aligned} \tag{2.4}$$

whose solution is obtained by simply replacing Σ_y with Σ'_y.

$$|\Delta y|^2_{\Sigma y'} = r^T \cdot \Sigma^{-1}_{y'} \cdot r \tag{2.5}$$

If the initial guess of the state is accurate enough, the GWLS method is capable of providing better estimates for the static-state vector.

2.2. Extended WLS

One major limitation of the GWLS method is that while it is able to take parameter uncertainty into account, it cannot identify the influence of each error causing on the final state, since in 2.3 the uncertainties of all three kinds of contribution are mixed together.

Therefore, in this section in order to further improve the effectiveness of SE, an extended WLS method (EWLS) will be considered. In this extended approach, the minimization is applied to the whole data error vector Σ_d rather than only the misfit r, which is the case in WLS and GWLS methods. Thus, the estimate problem becomes:

$$\begin{aligned} &\underset{x,\Delta d}{argmin} |\Delta d|^2_{\Sigma d} \\ &s.t. r = A(x;\pi)\Delta d \end{aligned} \tag{2.6}$$

Though not strictly necessary, in the EWLS scenario we also assume the parameter and measurement errors are entirely uncorrelated, like in the previous case. Thus, the variance-covariance matrix of the data vector Σ_d will be:

$$\Sigma_d = \begin{bmatrix} \Sigma y & 0_{M\times P} \\ 0_{P\times M} & \Sigma\pi \end{bmatrix} \in \mathbf{R}^{(M+P)\times(M+P)} \tag{2.7}$$

It is now possible to solve the constrained problem in 2.6, in which the unknown Δd is:

$$\Delta d = \Sigma_d A^T [A\Sigma_d A^T]^{-1} r \tag{2.8}$$

Note that since 2.8 expresses the data error δ_d as a function of x, the EWLS estimate of x can be found through the minimization of 2.6, which is the weighted squared norm of 2.8:

$$|\Delta d|^2_{\Sigma d} = r^T \cdot [A\Sigma_d A^T]^{-1} \cdot r \tag{2.9}$$

Considering how the matrix A is defined and the structure of the data variance-covariance matrix Σd, it can be seen that it will give an evaluation of the state identical to that

provided by GWLS, if using a same initial guess x_0.

However, the EWLS method is different from GWLS in that it recursively evaluates the matrix A with the newly-found kth state x_k. Thus, the previous approximated augmented measurement error 2.2 instead becomes:

$$\Delta y' \approx \Delta y - \left.\frac{\partial f}{\partial \pi^T}\right|_{xk,\pi} \cdot \Delta\pi - \frac{\partial}{\partial x^T}\left(\frac{\partial f}{\partial \pi^T}\Delta\pi\right)_{xk,\pi} \cdot \Delta x_k \tag{2.10}$$

As it uses an iterative state in the expression, the EWLS method will be more accurate than GWLS, especially in the case of a grossly wrong initial guess.

3 | Simulation Based on IEEE14 Bus System

In this chapter, a MATLAB test simulating the aforementioned SE methods is conducted. In this simulation, a detailed and adaptive power system model is established, which allows a flexible and suitably complex testing environment. Measurements involved in the simulation are generated synthetically with additional artificial errors. A Monte Carlo trial [4] is performed to test the effectiveness and robustness of the algorithms by introducing a large quantity of random samplings.

The trial can be broken down into the following parts:

- Input of true parameters π_t;
- Input of data uncertainty σ_y, σ_π, both for parameters and measurements;
- Input of an initial state guess x_0;
- True state of the system x_t, which is obtained through a traditional loadflow;
- True measurement set y_t, which is generated synthetically through links established between data and the state; A group of nominal parameters $\tilde{\pi}$ as well as measurements $\tilde{y}$ meant for the Monte Carlo trial, which are generated through an artificial perturbation related to the given uncertainty;
- Three estimators introduced in the previous chapters that are meant to be tested;
- Output of a group of resulting SE error $\delta\tilde{x} = \tilde{x} - x_t$, which can then be processed and analyzed.

A flowchart of the process is shown in 3.1.

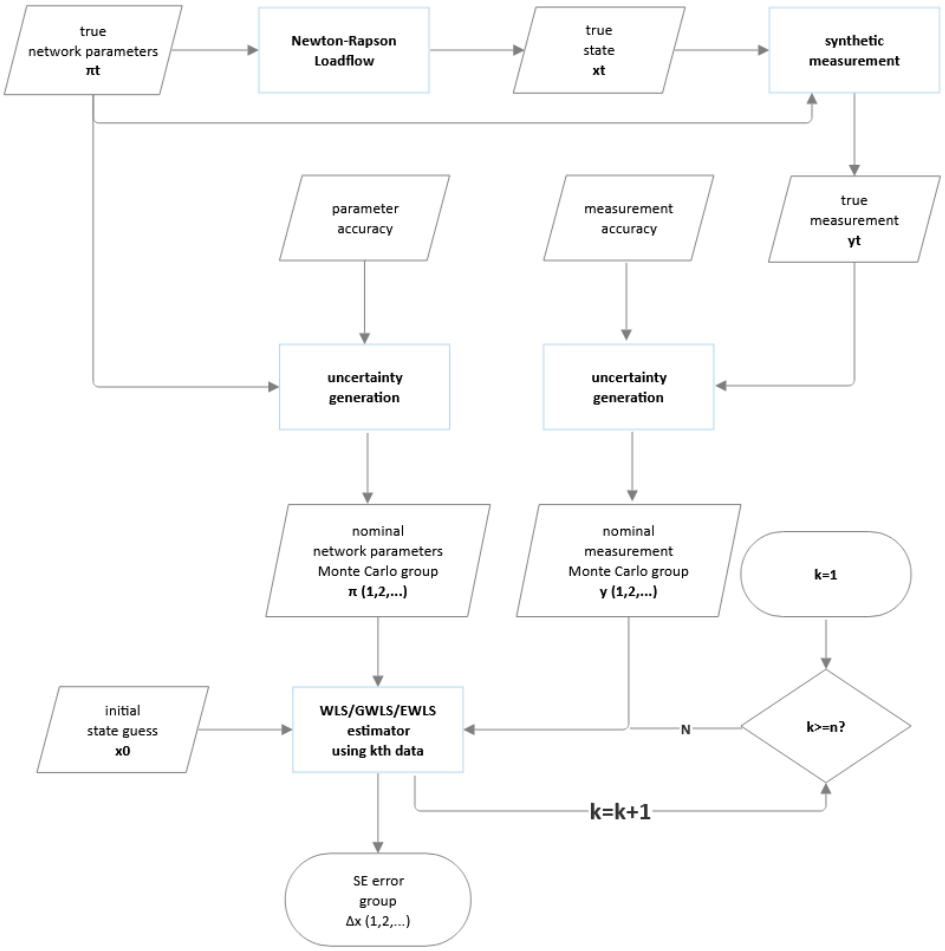

Figure 3.1: Simulation Process

3.1. IEEE14 Bus System

In this simulation, the IEEE14 bus system is chosen to represent the system in testing with its suitable complexity in mind, though the same algorithm may be easily extended to other similar power systems.

The IEEE14 bus system [15] [3] is an approximation of one portion of the American Electric Power System as of Feburary 1962, commonly used in power system testing. The system consists of 14 buses, to which 5 generators and 11 loads are connected, as shown in figure 3.2. Tap-changing transformers as well as shunt capacitors are also present in the network.

Network topology and corresponding parameter data provided by IEEE official data base

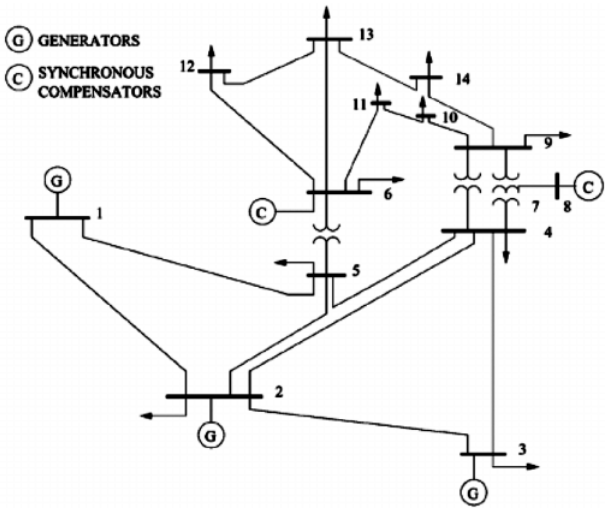

Figure 3.2: IEEE14 Bus System [15]

are considered "true" data $\tilde{\pi}_t$ and k_t of the actual system, while the later perturbed parameter data are considered nominal ones (i.e. the known parameter), for the sake of a simpler and less computationally expensive approach.

A total of 27 state variables are established in the 14 bus system:

$$\begin{aligned} x_{1 \text{ to } 14}&: \text{Voltage magnitude on 14 buses} \\ \theta_{1 \text{ to } 13}&: \text{phase on 13 buses (excluding bus 1)} \end{aligned} \tag{3.1}$$

Reading from the data of 20 transmission lines composing the system and excluding those with a value of 0 (assuming the 0 in the datasheet means the lack of this specific property and is thus certain), a total of 42 parameter data that are subject to uncertainty can be extracted from the 14 bus system:

$$\begin{aligned} R_{1 \text{ to } 20}&: \text{Resistance on 15 lines} \\ X_{1 \text{ to } 20}&: \text{Reactance on 20 lines} \\ B_{1 \text{ to } 20}&: \text{Half-line capacity on 7 lines} \end{aligned} \tag{3.2}$$

As mentioned before, the topology k itself is taken as absolute. Also note that while tap-changing transformer values a and shunt capacitors may also possess an uncertain nature, they are considered perfect here in order to give a more evident and straightforward analysis.

For a full report on the data of the network, see appendix C.

3.2. Newton-Rapson Loadflow

In order to obtain the state of the simulated system, a loadflow must be performed. Newton-Rapson method is chosen for its decent robustness and widespread use.

Considering this:

$$f(x_t) = f(x + \Delta x) = 0 \tag{3.3}$$

In which $f(x)$ is the "measurement set" function of the state, though in a loadflow the only measurements available are the given real as well as reactive power, obtained through the knowledge of generators and loads installed in the system.

Using Taylor's expansion to isolate the part contributed by error Δx:

$$f(x + \Delta x) \approx f(x) + \left(\frac{\partial f}{\partial x^T}\right) \Delta x = 0 \tag{3.4}$$

This equation can then be used in an iterative form:

$$\Delta x_k = -\left(\frac{\partial f}{\partial x^T}\right)^{-1}_{x_k} f(x_k) \tag{3.5}$$

Where

$$x_{k+1} = x_k + \Delta x_k \tag{3.6}$$

The iteration will be repeated until Δx is lower than a pre-defined threshold, after which the state obtained can be considered a very good reflection of the given system data. Since the system data is treated as perfect, this obtained result would be considered the true state of the system $\tilde{x}_t$, which will then be used to calculate the synthetic measurements, as well as serve as a indicator for the evaluation of the final results.

$$\begin{aligned} &x_{t1 \text{ to } 14}\text{: Voltage magnitude on 14 buses} \\ &\theta_{t1 \text{ to } 13}\text{: phase on 13 buses (excluding bus 1)} \end{aligned} \tag{3.7}$$

3.3. Synthetic Measurements

After the true state of the system is established, a certain measurement set must be chosen in order to feed the estimator its required information. The specific measurement set must be chosen in a way such that the observability [14] [10] [21] of every state variable can be assured. In addition, a level of redundancy must be available as SE method relies on it to be effective. Moreover, as the IEEE14 bus system is meant to approximately represent a real-life power system, the actual availability of the chosen "synthetic" measurements should also be taken into consideration.

To achieve those goals, seven types of different measured data are used in the test, which are obtained in the following ways:

- Voltage magnitude squared:

$$A_1 = \left|\overline{V_\mathrm{i}}\right|^2 = \overline{V_\mathrm{i}}\overline{V_\mathrm{i}}^* = x_\mathrm{i}e^{j\theta_\mathrm{i}} * x_\mathrm{i}e^{-j\theta_\mathrm{i}} = x_\mathrm{i}^2 \tag{3.8}$$

- Magnitude squared of current flow in-line:

$$A_2 = \left|\overline{I_\mathrm{ij}}\right|^2 = \overline{I_\mathrm{ij}I_\mathrm{ij}}^* \tag{3.9}$$

  Where the current flow in-line $\overline{I_\mathrm{ij}}$ would be:

$$\overline{I_\mathrm{ij}} = \frac{\overline{V_\mathrm{i}} - \overline{V_\mathrm{j}}}{R_\mathrm{k} + jX_\mathrm{k}} + jB_\mathrm{k}\overline{V_\mathrm{i}} = \frac{x_\mathrm{i}e^{j\theta_\mathrm{i}} - x_\mathrm{j}e^{j\theta_\mathrm{j}}}{R_\mathrm{k} + jX_\mathrm{k}} + jB_\mathrm{k}x_\mathrm{i}e^{j\theta_\mathrm{i}} \tag{3.10}$$

- Magnitude squared of current injected on buses:

$$A_3 = \left|\sum_{j=1}^{n}\overline{I_\mathrm{ij}}\right|^2 = \sum_{j=1}^{n}\overline{I_\mathrm{ij}}\sum_{j=1}^{n}\overline{I_\mathrm{ij}}^* \tag{3.11}$$

- Active power flow in-line:

$$A_4 = P_\mathrm{ij} = \mathrm{Real}(\overline{S_\mathrm{ij}}) = \mathrm{Real}(\overline{V_\mathrm{i}I_\mathrm{ij}^*}) \tag{3.12}$$

- Reactive power flow in-line:

$$A_5 = Q_{\mathrm{ij}} = \mathrm{Imag}(\overline{S_{\mathrm{ij}}}) = \mathrm{Imag}(\overline{V_{\mathrm{i}} I_{\mathrm{ij}}^*}) \tag{3.13}$$

- Active power injected on buses:

$$A_6 = P_k = \sum_{j=1}^{n} P_{\mathrm{kj}} \tag{3.14}$$

- Reactive power injected on buses:

$$A_7 = Q_k = \sum_{j=1}^{n} Q_{\mathrm{kj}} \tag{3.15}$$

Lists of different measurement sets concerning types, locations as well as the significance of their data uncertainty can then be made to accommodate the needs of various cases.

3.4. Uncertainty Generation

Knowing the true parameter and measurement data, it is then possible to perturb them randomly by a given standard deviation σ_y to obtain "known" data, which include an artificial error the SE method is meant to eliminate.

$$\begin{aligned} y &= y_t + \Delta y \\ \pi &= \pi_t + \Delta \pi \end{aligned} \tag{3.16}$$

Though not necessarily true, errors in the data are considered jointly independent, thus obtaining a variance-covariance matrix with all covariance equal to zero:

$$\Sigma_y = \begin{bmatrix} \sigma_{y1}^2 & 0 & 0 & 0 \\ 0 & \sigma_{y2}^2 & & \\ 0 & & \ldots & \\ 0 & & & \sigma_{ym}^2 \end{bmatrix} \tag{3.17}$$

The variance-covariance matrix for parameters can be obtained in a similar way:

$$\Sigma_\pi = \begin{bmatrix} \sigma_{\pi 1}^2 & 0 & 0 & 0 \\ 0 & \sigma_{\pi 2}^2 & & \\ 0 & & \dots & \\ 0 & & & \sigma_{\pi n}^2 \end{bmatrix} \tag{3.18}$$

3.5. Jacobian Matrices

Jacobian matrices on measurement data with respect to their uncertain components are necessary for the SE methods to deduce how uncertain the resulting state will be. For the classical WLS estimator, a Jacobian matrix with respect to state variables is enough:

$$H_1 = \begin{bmatrix} \frac{\partial f_1}{\partial x_1} & \dots & \frac{\partial f_1}{\partial x_n} & \frac{\partial f_1}{\partial \theta_1} & \dots & \frac{\partial f_1}{\partial \theta_{n-1}} \\ \dots & & & & & \dots \\ \frac{\partial f_m}{\partial x_1} & \dots & & & & \frac{\partial f_m}{\partial \theta_{n-1}} \end{bmatrix} \tag{3.19}$$

On the other hand, an additional Jacobian matrix with respect to the uncertain parameters must be made for GWLS and EWLS estimators, as they need to evaluate their influence on the state:

$$H_2 = \begin{bmatrix} \frac{\partial f_1}{\partial R_1} & \dots & \frac{\partial f_1}{\partial R_n} & \frac{\partial f_1}{\partial X_1} & \dots & \frac{\partial f_1}{\partial X_n} & \frac{\partial f_1}{\partial B_1} & \dots & \frac{\partial f_1}{\partial B_n} \\ \dots & & & & & & & & \\ \frac{\partial f_m}{\partial R_1} & & & & \dots & & & & \frac{\partial f_m}{\partial B_n} \end{bmatrix} \tag{3.20}$$

For a full report on derivatives covering all types of measurements with respect to state variables as well as parameters, see appendix A and B.

3.6. WLS Estimator

WLS estimator can then use an iterative procedure to estimate the true state using only the "known" data and parameters. Each iteration includes the following steps:

Recalculating the data Jacobian with respect to state variables using the latest state estimate:

$$H_1 = \begin{bmatrix} \frac{\partial f_1}{\partial x_1} & \cdots & \frac{\partial f_1}{\partial x_n} & \frac{\partial f_1}{\partial \theta_1} & \cdots & \frac{\partial f_1}{\partial \theta_{n-1}} \\ \cdots & & & & & \cdots \\ \frac{\partial f_m}{\partial x_1} & \cdots & & & & \frac{\partial f_m}{\partial \theta_{n-1}} \end{bmatrix}_{\tilde{x}_k, \tilde{\pi}} \tag{3.21}$$

Where k is the iterating times. Note that since WLS does not take parameters into consideration, it always uses the given π thinking it is perfect.

Calculating the gain matrix:

$$G_{\tilde{x}_k} = \left(\frac{\partial f}{\partial \tilde{x}}\right)^T_{\tilde{x}_k, \pi} \Sigma_y^{-1} \left(\frac{\partial f}{\partial \tilde{x}}\right)_{\tilde{x}_k, \pi} \tag{3.22}$$

Obtaining the iterative modifier to the state:

$$\Delta \tilde{x}_k = G_{\tilde{x}_k}^{-1} \left(\frac{\partial f}{\partial \tilde{x}}\right)_{\tilde{x}_k, \pi} \Sigma_y^{-1} \tilde{r}_k \tag{3.23}$$

Where the residue $\tilde{r}$ is obtained by comparing the inaccurate data $\tilde{y}$ and an iterating y_k derived from the existing state estimate:

$$\tilde{r}_k = \tilde{y} - f(x_k; \pi) \tag{3.24}$$

Finally, adding the modifier to the state obtained in the last iteration:

$$\tilde{x}_{k+1} = \tilde{x}_k + \Delta \tilde{x}_k \tag{3.25}$$

3.7. GWLS Estimator

The GWLS method is different to WLS only in that instead of directly using the variance-covariance matrix Σ_y it uses a modified $\Sigma_{y'}$, which also considers the impact of parameter uncertainty:

$$\Sigma'_y = \Sigma_y + \left(\frac{\partial f}{\partial \pi}\right)_{x_0, \pi} \Sigma_\pi \left(\frac{\partial f}{\partial \pi}\right)^T_{x_0, \pi} \tag{3.26}$$

Where the derivatives with respect to π need to be computed in addition to state Jacobian:

$$H_2 = \begin{bmatrix} \frac{\partial f_1}{\partial R_1} & \cdots & \frac{\partial f_1}{\partial R_n} & \frac{\partial f_1}{\partial X_1} & \cdots & \frac{\partial f_1}{\partial X_n} & \frac{\partial f_1}{\partial B_1} & \cdots & \frac{\partial f_1}{\partial B_n} \\ \cdots & & & & & & & & \\ \frac{\partial f_m}{\partial R_1} & & & & \cdots & & & & \frac{\partial f_m}{\partial B_n} \end{bmatrix} \tag{3.27}$$

It is worth noting that this modified matrix is only calculated once at the beginning of the algorithm. Therefore, the Jacobian with respect to parameters are only computed with the initial guess $\tilde{x}_0$. Should a terrible guess be given initially the robustness of GWLS can be heavily impacted.

3.8. EWLS Estimator

In the extended approach the Jacobian with respect to parameters is computed each iteration. In the place of Σ_y an intermediate matrix Q is calculated:

$$Q = A\Sigma_d A^T \tag{3.28}$$

Where

$$A = [I_M - \left(\frac{\partial f}{\partial \pi}\right)_{x_k,\pi}] \tag{3.29}$$

And

$$\Sigma d = \begin{bmatrix} \Sigma y & 0_{M\times P} \\ 0_{P\times M} & \Sigma \pi \end{bmatrix} \in \mathbf{R}^{(M+P)\times(M+P)} \tag{3.30}$$

In this way, the impact of parameter uncertainty on the state is revised at each iteration, minimizing the possible bias.

3.9. Finishing Criteria

A minimum modifier $\tilde{x}_{\min}$ is set for each estimator. Should the resulting $\tilde{x}_k$ is less than it, the iteration is immediately dropped and the final state is seen as the resulting estimate.

Following the completion of a Monte Carlo trial, a very large number of obtained results will form a group to be analyzed in detail.

4 | Case Studies

In this chapter, various cases are tested to verify the effectiveness and robustness between WLS, GWLS as well EWLS methods, each under a specific circumstance. Both graphs and statistical tests are used to analyze the obtained results further.

A total of 4 cases are reported:

- Case 1: An "ideal" system model with only measurement data error is used. In this case both WLS and EWLS provide the same result;
- Case 2: A parameter uncertainties are introduced, where WLS provides an inconsistent estimate while EWLS is correct;
- Case 3: A different measurement set with worse network observability is adopted, which WLS produces awful results, but EWLS can still keep up;
- Case 4: GWLS and EWLS methods are compared to show how a bad initial guess can affect GWLS greatly. The pros and cons of both methods are also briefly discussed.

All cases are based on the IEEE14 bus system.

4.1. Case 1

In the first case, only a realistically small error is present in the measurement data, while parameters are considered almost perfect.

- Measurement standard deviation $\sigma_y = 0.01$ p.u.
- Parameter standard deviation $\sigma_\pi = 10^{-6}\ \pi^T$

Considering the estimators requires a good observability of the entire system to work properly [8] [12], a set of 41 different measurements is carefully chosen in a way that they may fully cover the information need of all 27 variables, while still be able to reflect clearly the differences between estimator methods.

Measurement Type	Measurements used
Voltage magnitude	1
Active power injection	8
Reactive power injection	8
Active power flow	12
Reactive power flow	12

Table 4.1: Measurement Set, Case 1

A sufficiently good initial guess $\tilde{x}_0$ is important for evaluating the effectiveness of estimators since:

- They take less time to converge;
- A grossly bad guess may stop the algorithm from converging definitely;
- GWLS suffers greatly from the inaccuracy of the initial guess, which will be demonstrated in case 4.

Assuming firstly:

- Voltage magnitude $x_{1 \text{ to } 14} = 1$
- Voltage phase $\theta_{1 \text{ to } 13} = 0$

Under this assumption, one single WLS iteration is performed to obtain the following result:

$x_{1 \text{ to } 14}$	$\theta_{1 \text{ to } 13}$
1.0379	
1.0222	-0.1006
0.9818	-0.2496
0.9835	-0.2017
0.9853	-0.172
1.026	-0.2871
1.024	-0.2524
1.056	-0.2521
1.0173	-0.2821
1.0109	-0.2891
1.0142	-0.292
1.01	-0.3055
1.003	-0.3088
0.9921	-0.3136

Table 4.2: Initial State Guess $\tilde{x}_0$, Case 1

This obtained state is used as the input for the estimator test below, in order to ensure the algorithm can work in converging state.

A 1000-time Monte Carlo trial is performed for WLS and EWLS methods, assuming zero mean and variance defined above.

The results are shown in figure 4.1 using the magnitude and phase of bus 2 as an example.

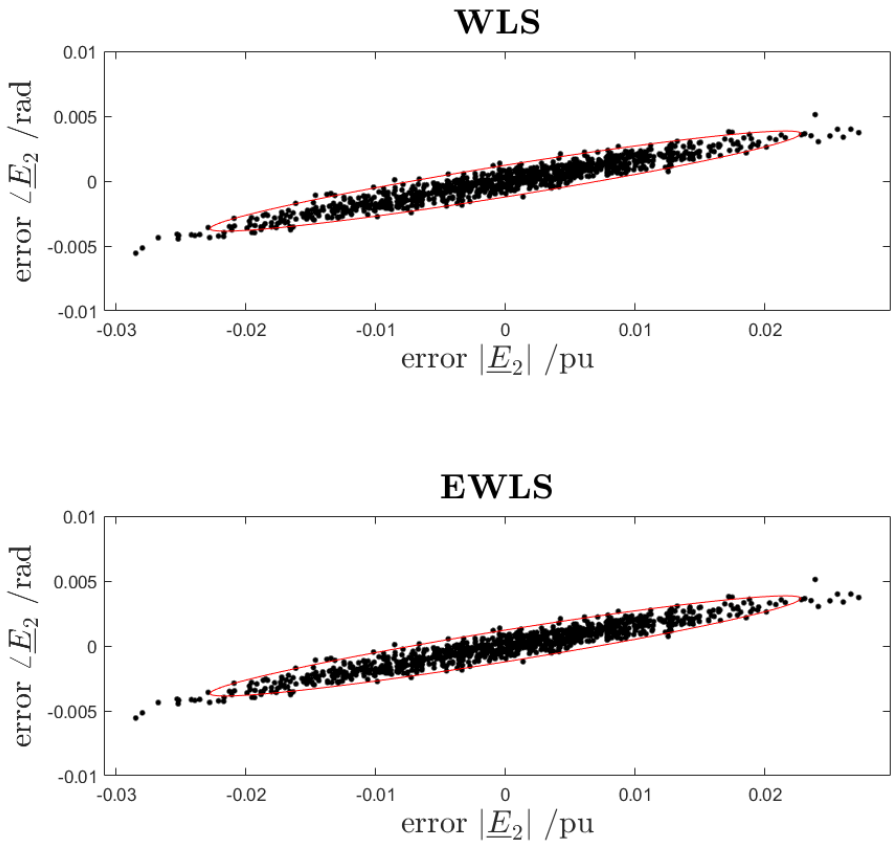

Figure 4.1: Voltage-phase Error of Bus 2 -Case 1

A scatter plot is drawn to show the statistical distribution of the errors of estimated state variables in the 1000-time trial. The red ellipses indicate the predicted variance of the state variable provided by the corresponding estimator in its 1st trial, with a 0.95 confidence level.

It can be observed that with a near-perfect knowledge of parameters both methods are able to obtain a good prediction on the results, with most of the estimates landing within the variance zones.

Sampling std. dev. $s_{\tilde{x}WLS}$	Computed std. dev. $\sigma_{\tilde{x}WLS}$	Sampling std. dev. $s_{\tilde{x}EWLS}$	Computed std. dev. $\sigma_{\tilde{x}EWLS}$
0.0016	0.0016	0.0016	0.0016
0.0042	0.0040	0.0042	0.0040
0.0035	0.0033	0.0035	0.0033
0.0030	0.0029	0.0030	0.0029
0.0051	0.0049	0.0051	0.0049
0.0046	0.0045	0.0046	0.0045
0.0049	0.0048	0.0049	0.0048
0.0053	0.0050	0.0053	0.0050
0.0052	0.0050	0.0052	0.0050
0.0052	0.0050	0.0052	0.0050
0.0055	0.0053	0.0055	0.0053
0.0055	0.0053	0.0055	0.0053
0.0057	0.0054	0.0057	0.0054
0.0093	0.0092	0.0093	0.0092
0.0094	0.0093	0.0094	0.0093
0.0097	0.0096	0.0097	0.0096
0.0095	0.0094	0.0095	0.0094
0.0095	0.0094	0.0095	0.0094
0.0104	0.0091	0.0104	0.0091
0.0097	0.0092	0.0097	0.0092
0.0096	0.0091	0.0096	0.0091
0.0098	0.0093	0.0098	0.0093
0.0100	0.0093	0.0100	0.0093
0.0104	0.0092	0.0104	0.0092
0.0107	0.0093	0.0107	0.0093
0.0107	0.0094	0.0107	0.0094
0.0104	0.0095	0.0104	0.0095

Table 4.3: Sampling and Computed Standard Deviation, WLS/EWLS, Case 1

Figure 4.3 shows the sampling and computed standard deviations $s_{\tilde{x}}$, $\sigma_{\tilde{x}}$ of all 27 state

variables obtained in case 1, for both WLS and EWLS methods. Since the statically and analytically obtained results are largely consistent with each other, it may be said that with only measurement errors present in the observation both WLS and EWLS can provide unbiased results.

4.2. Case 2

Case 2 includes a parameter error with a standard deviation $\sigma_\pi = 0.15/\sqrt{3}\ \pi^T$, while the measurement error is kept the same with case 1.

- Measurement standard deviation $\sigma_y = 0.01$ p.u.
- Parameter standard deviation $\sigma_\pi = 0.0866\ \pi^T$

The measurement set $\tilde{y}$, initial state guess $\tilde{x}_0$ and times of Monte Carlo trial are also the same as are used in case 1 in order to be comparative.

The resulting scatter plots as well as estimated variance are reported in figure 4.2, again using bus 2 as an example.

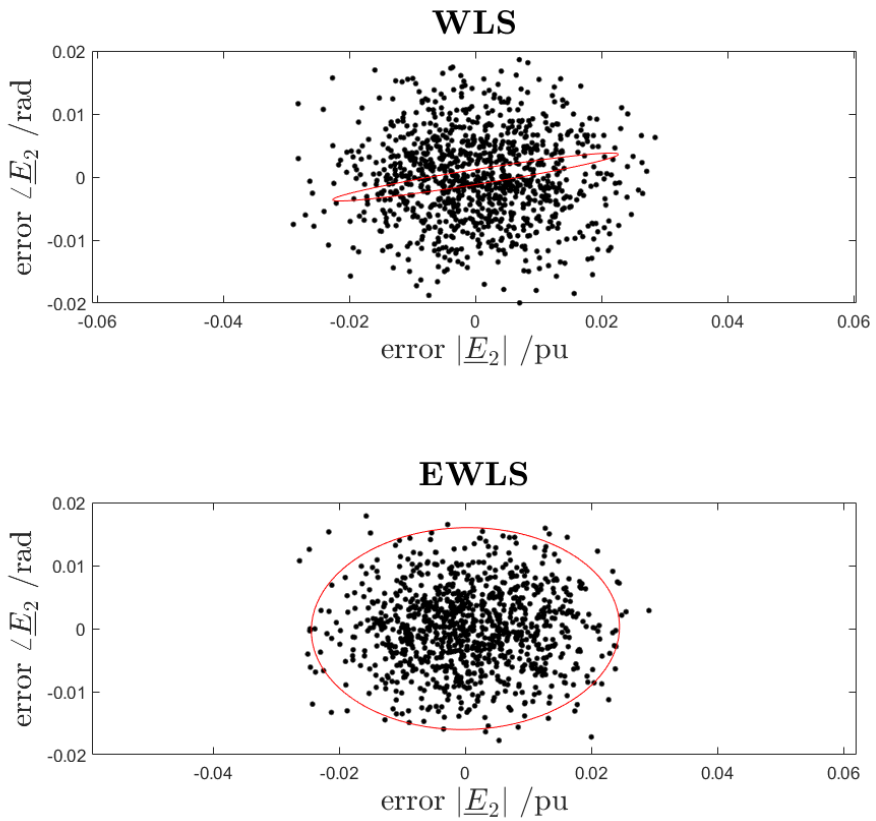

Figure 4.2: Voltage-phase Error of Bus 2 -Case 2

This time there is a drastic difference between the two methods. While EWLS retains the ability to identify the error contribution to the state from data uncertainty, WLS method gives a gross underestimate of the state variance. Actually, in the case of WLS, most of the state variable errors land outside the region of the algorithm's designation.

Another interesting thing to point out is that the variance prediction on the phase θ_2 is even more terrible than on the magnitude x_2. The cause of this phenomenon is that phases' sensitivities on parameter error are often higher than those of magnitudes, as there are no direct measurements on them included in this case.

A more extreme contrast can be observed using the phase error of bus 5 as an example.

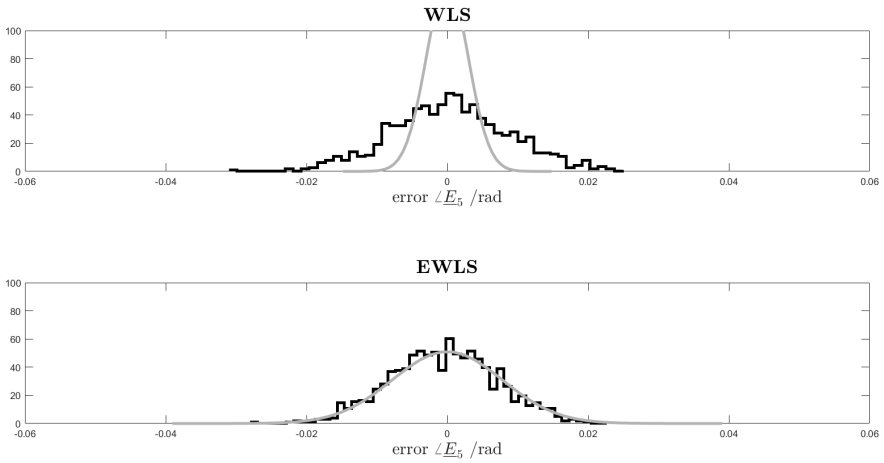

Figure 4.3: Phase Error PDF of Bus 6 -Case 2

Figure 4.3 shows the PDF of the phase error produced in the Monte Carlo trial. The gray curve indicates the computed standard deviation σ_θ of the estimators with a 0.95 confidence level.

Clearly, in the case of WLS, variance of the state is significantly underestimated. Instead, the variance provided by EWLS well aligns with the pdf of its errors produced in the trial. EWLS also has a thinner spread out than WLS, showing it has a better capability handling the uncertainty.

Sampling std. dev. $s_{\tilde{x}WLS}$	**Computed std. dev.** $\sigma_{\tilde{x}WLS}$	**Sampling std. dev.** $s_{\tilde{x}EWLS}$	**Computed std. dev.** $\sigma_{\tilde{x}EWLS}$
0.0072	0.0015	0.0067	0.0066
0.0104	0.0039	0.0087	0.0084
0.0087	0.0030	0.0081	0.0079
0.0087	0.0026	0.0080	0.0079
0.0115	0.0045	0.0098	0.0097
0.0096	0.0042	0.0089	0.0088
0.0098	0.0046	0.0091	0.0090
0.0099	0.0048	0.0093	0.0091
0.0098	0.0048	0.0092	0.0091
0.0105	0.0047	0.0094	0.0094
0.0118	0.0050	0.0100	0.0100
0.0117	0.0049	0.0100	0.0101
0.0103	0.0052	0.0096	0.0095
0.0098	0.0092	0.0094	0.0095
0.0105	0.0094	0.0100	0.0102
0.0112	0.0097	0.0107	0.0107
0.0106	0.0095	0.0102	0.0104
0.0106	0.0095	0.0102	0.0104
0.0117	0.0092	0.0111	0.0101
0.0109	0.0094	0.0105	0.0103
0.0110	0.0092	0.0107	0.0104
0.0110	0.0094	0.0106	0.0103
0.0112	0.0094	0.0108	0.0103
0.0116	0.0093	0.0111	0.0102
0.0120	0.0094	0.0114	0.0104
0.0121	0.0095	0.0115	0.0104
0.0117	0.0096	0.0112	0.0106

Table 4.4: Sampling and Computed Standard Deviation, WLS/EWLS, Case 2

Again, figure 4.4 shows the sampling and computed standard deviations $s_{\tilde{x}}$, $\sigma_{\tilde{x}}$ of all 27

state variables obtained in case 2. Now, with uncertain paramter as input, it can be seen that the computed standard deviations of WLS are very terrible reflections of the actual sampling deviations. In fact, with regard to phases, WLS's estimate often only account for less than 0.3 of the actual values.

On the other hand, EWLS provides results quite close to the sampling values, confirming the results previously concluded by the plots.

4.3. Case 3

Case 3 uses the same data uncertainty set as case 2.

- Measurement standard deviation $\sigma_y = 0.01$ p.u.
- Parameter standard deviation $\sigma_\pi = 0.0866\ \pi^T$

Instead case 3 uses a different measurement set as the input. This time, a total of 49 measurements.

Measurement Type	Measurements used
Voltage magnitude	5
Current flow	5
Current injection	5
Active power injection	6
Reactive power injection	6
Active power flow	11
Reactive power flow	11

Table 4.5: Measurement Set, Case 3

The voltage and phase of bus 2 are used again as an example, drawing an 2D scatter plot as is shown in 4.4.

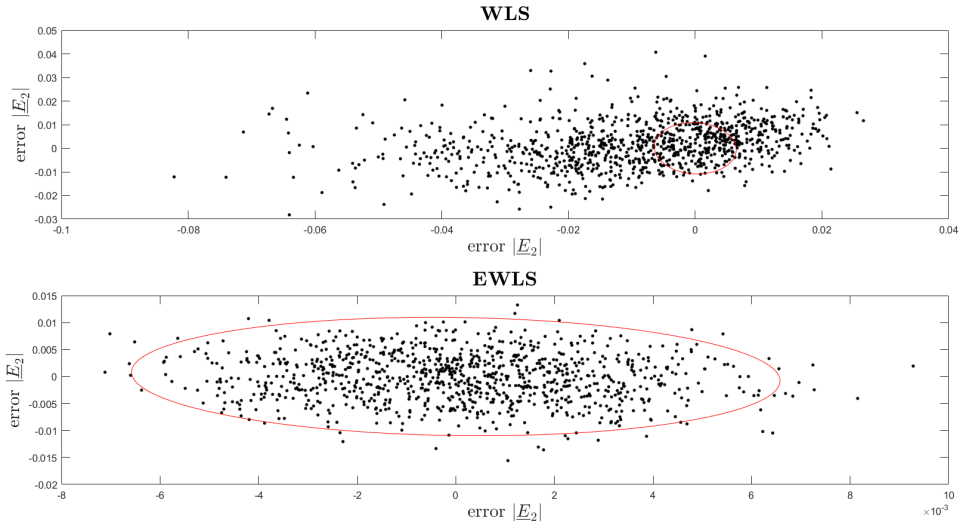

Figure 4.4: Voltage-phase Error of Bus 2 -Case 2

It can be observed that despite the increase of measurement number, the performance of WLS has reduced. The error distribution from Monte Carlo trial has a larger spread out

than in the previous case. The red ellipse indicating the estimator's predicted variance only contains a small portion of the estimates, showing a very high inaccuracy. There are also a few gross errors that lie very far from the group, which are outright unusable.

On the other hand, EWLS method still performs admirably. Looking at the axis scales it can be observed that the error spread out of EWLS are actually several decimals ahead of WLS. The estimated variance with a 0.95 confidence level also includes most of the trial results, indicating a good prediction. Further more, large errors are fewer both in number and gravity compared to WLS method.

The causes of this phenomenon are several:

- Firstly, the choice of location for this measurement set gives a worse observability of the state than the previous case, for which WLS method has a hard time exploiting the abundance of data;
- Current measurements are heavily impacted by parameter uncertainty. The inclusion of them makes WLS very terrible at utilizing the data. Actually, in a few cases the addition of current measurements can negatively affect the performance of WLS. EWLS, however, does not have this problem since it already account for the parameter errors.

4.4. Case 4

Case 4 uses the same inputs of case 2, but instead gives a comparison between GWLS and EWLS methods.

- Measurement standard deviation $\sigma_y = 0.01$
- Parameter standard deviation $\sigma_\pi = 0.0866$

If the previous initial guess is used, the following result can be obtained:

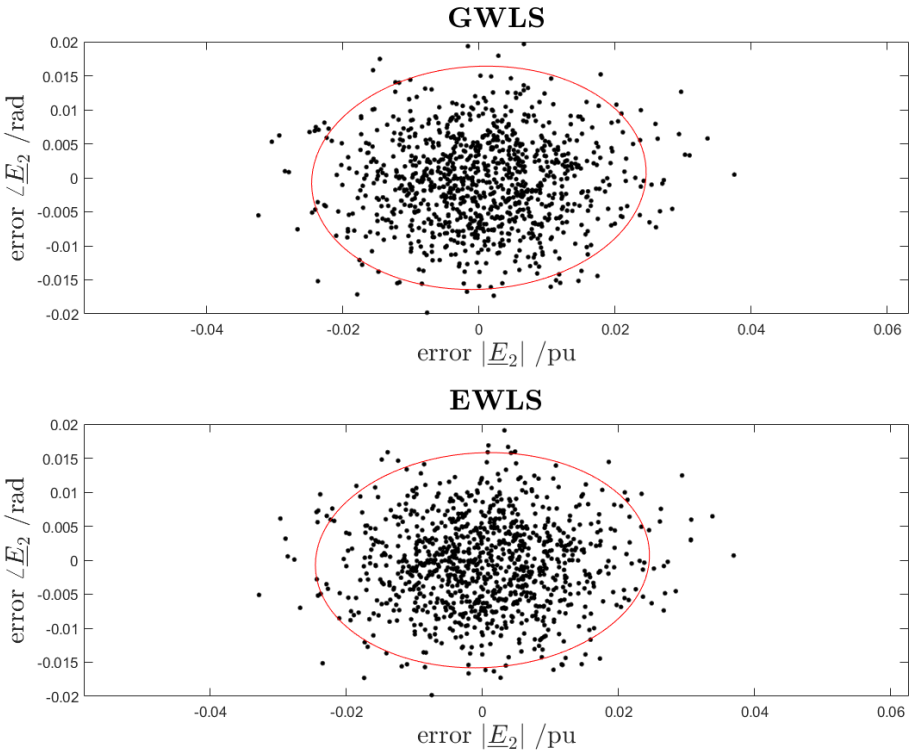

Figure 4.5: Voltage-phase Error of Bus 2 -Case 4

Since the estimate is based on a relatively good guess, the difference is not immediately obvious as shown in figure 4.5. In either case, most of the errors land in the predicted variance ellipse, and the spread out is similar. It would appear that GWLS and EWLS both have good handling on the parameter uncertainty.

In fact, if we compare the standard deviations obtained in the trial:

Sampling std. dev. $s_{\tilde{x}GWLS}$	**Computed std. dev.** $\sigma_{\tilde{x}GWLS}$	**Sampling std. dev.** $s_{\tilde{x}EWLS}$	**Computed std. dev.** $\sigma_{\tilde{x}EWLS}$
0.0066	0.0067	0.0066	0.0065
0.0083	0.0090	0.0083	0.0084
0.0077	0.0083	0.0078	0.0078
0.0077	0.0082	0.0078	0.0077
0.0097	0.0102	0.0098	0.0097
0.0086	0.0092	0.0086	0.0088
0.0087	0.0094	0.0087	0.0090
0.0089	0.0095	0.0089	0.0091
0.0090	0.0095	0.0090	0.0091
0.0093	0.0098	0.0094	0.0094
0.0100	0.0105	0.0100	0.0100
0.0101	0.0105	0.0101	0.0101
0.0094	0.0100	0.0095	0.0095
0.0097	0.0095	0.0097	0.0095
0.0103	0.0100	0.0103	0.0100
0.0109	0.0107	0.0109	0.0106
0.0105	0.0103	0.0105	0.0103
0.0105	0.0103	0.0105	0.0103
0.0114	0.0100	0.0114	0.0099
0.0108	0.0101	0.0108	0.0101
0.0110	0.0103	0.0110	0.0102
0.0109	0.0102	0.0109	0.0102
0.0111	0.0102	0.0111	0.0101
0.0113	0.0101	0.0113	0.0100
0.0116	0.0103	0.0116	0.0102
0.0118	0.0103	0.0118	0.0102
0.0114	0.0104	0.0114	0.0104

Table 4.6: Sampling and Computed Standard Deviation, GWLS/EWLS, Case 4

Table 4.6 shows that despite some differences between GWLS and EWLS estimates can be observed, the computed standard deviations $\sigma_{\tilde{x}}$ from both methods still cling relatively close to the actual sampling values, unlike WLS in the previous cases which performed terribly.

However, if we perform the Monte Carlo trial instead with a relatively bad initial state as the following:

$x_{1 \text{ to } 14}$	$\theta_{1 \text{ to } 13}$
1.061	
1.062	0
1.063	-0.01
1.064	-0.02
1.065	-0.03
1.066	-0.04
1.067	-0.05
1.068	-0.06
1.069	-0.07
1.07	-0.08
1.071	-0.09
1.072	-0.1
1.073	-0.11
1.074	-0.12

Table 4.7: Bad Initial Guess $\tilde{x}_0$

Plotting again the scatter graph for bus 2 from the results:

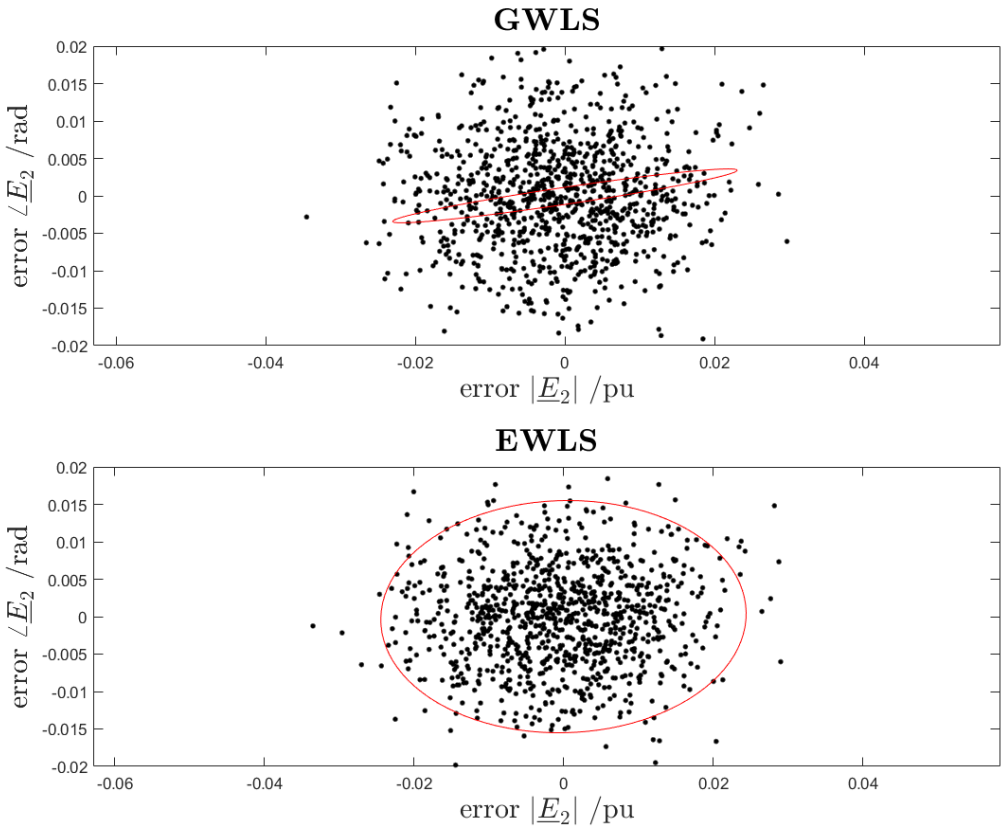

Figure 4.6: Voltage-phase Error of Bus 2, with Bad Initial Guess -Case 4

From figure 4.6 it can be seen that GWLS is heavily biased just like WLS was, with its computed variance heavily underestimated. As is mentioned in the previous chapters, GWLS algorithm calculates the impact of parameter uncertainty only with regard to the initial state guess. This means the effectiveness of GWLS will degrade with large initial guess deviates off the actual state.

Sampling std. dev. $s_{\tilde{x}GWLS}$	Computed std. dev. $\sigma_{\tilde{x}GWLS}$	Sampling std. dev. $s_{\tilde{x}EWLS}$	Computed std. dev. $\sigma_{\tilde{x}EWLS}$
0.0075	0.0015	0.0068	0.0063
0.0103	0.0042	0.0083	0.0084
0.0088	0.0035	0.0080	0.0077
0.0087	0.0031	0.0078	0.0076
0.0118	0.0052	0.0097	0.0099
0.0101	0.0051	0.0090	0.0088
0.0102	0.0055	0.0091	0.0090
0.0102	0.0057	0.0093	0.0092
0.0102	0.0057	0.0093	0.0092
0.0106	0.0058	0.0094	0.0095
0.0120	0.0065	0.0100	0.0101
0.0122	0.0069	0.0101	0.0102
0.0108	0.0064	0.0097	0.0096
0.0094	0.0093	0.0094	0.0094
0.0100	0.0094	0.0100	0.0100
0.0108	0.0098	0.0107	0.0106
0.0103	0.0095	0.0102	0.0102
0.0103	0.0095	0.0102	0.0102
0.0110	0.0102	0.0112	0.0098
0.0106	0.0094	0.0105	0.0101
0.0107	0.0093	0.0106	0.0102
0.0108	0.0095	0.0107	0.0101
0.0108	0.0096	0.0109	0.0101
0.0110	0.0099	0.0111	0.0100
0.0114	0.0108	0.0115	0.0101
0.0114	0.0110	0.0116	0.0101
0.0111	0.0102	0.0112	0.0103

Table 4.8: Sampling and Computed Standard Deviation with Bad Initial Guess, GWLS/EWLS, Case 4

As is shown in table 4.8, many of the computed deviations from GWLS are no longer in line, sometimes at around only 0.5 of the actual values. However, even with a relatively awful initial guess, EWLS is still capable of containing the parameter uncertainty and provides reasonable estimates, though more iteration times are required.

On the other hand, it may be said that GWLS is still a valid option when the deviance between the given and true state is small. Since GWLS only computes state derivatives with respect to parameter data only in the beginning of the algorithm while EWLS will repeatedly renew them according to the iterating state, a significant amount of computational efforts can be saved if a greater accuracy isn't necessary. It is also possible to switch to GWLS when the state is believed to be converging closely to its true values to save computing time should it be a concern.

However, since GWLS merges the impact of parameter errors into the variance-covariance matrix of measurements Σ_y, further analysis on the error contribution as well as bad data will not be possible, in which case EWLS must be used.

5 | Conclusions and Future Developments

5.1. Conclusions

In this thesis, novel WLS approaches in power system state estimation, meant to account for uncertain parameters which are not present in the classical model, are examined by both theoretical analysis and simulation tests.

A complex bus system model is first established, able to simulate generators, loads, tap-changing transformers, shunt capacitors as well as other components presented in a typical test network. Various types of measurements are also modelled to reflect a more practical environment. For this thesis' purpose, IEEE14 bus system is chosen for the simulation, though similar systems may be modelled in without much efforts.

Monte Carlo trials are deployed to give a deeper and statistical analysis to the aforementioned methods. Using a large number of trials it is possible to obtain the statistical distribution of estimate errors, reflecting the effectiveness and robustness of used algorithms.

It can then be proven that while the classical WLS method has the advantage of giving a more straightforward model and requiring less computational efforts, it does not perform well under circumstances where the given parameter data are inaccurate. Considering how measurement instruments are evolving quickly nowadays, this particular flaw may become even more problematic due to the rising relative contribution of parameter uncertainty to the final state estimate.

In order to solve this problem, a generalization of the classical WLS method is given to merge parameter uncertainty into the existing variance-covariance matrix. This method is relatively simple and requires little computational efforts to be added, however, it still has two major issues:

- GWLS relies on an accurate initial state to gain good estimates

- GWLS does not distinguish parameter uncertainty contribution from measurement, thus make it impossible to further analyze the data obtained.

EWLS is introduced to help with those issues. Rather than merging the uncertainty, EWLS instead takes those two uncertainty separately and re-computes their contribution for each iteration. It is proven to be capable of better utilizing the overabundance of data as SE methods originally intended, significantly outperforming WLS in several scenarios. Furthermore, EWLS is also able to properly formulate the error contributions from those two sources which GWLS cannot, providing an opportunity to examine bad data within even further.

5.2. Future Developments

While the ending results show a good indication of the effectiveness of the proposed methods, certain aspects of the work merit further investigations:

- Both the effectiveness and the computational efforts required varies depending on the measurement set chosen. Different types, location group, as well as numbers of measurements can all affect EWLS' capabilities on identifying the contribution of parameter uncertainty.
- Though EWLS provides opportunity for further analysis of the data, specific details of bad data detection requires future work to be done.

Bibliography

[1] H. Ahmadi and M. Armstrong. Transmission line impedance calculation using detailed line geometry and hem soil resistivity measurements. In *2016 IEEE Canadian Conference on Electrical and Computer Engineering (CCECE)*, pages 1–4, 2016. doi: 10.1109/CCECE.2016.7726808.

[2] M. Bockarjova and G. Andersson. Transmission line conductor temperature impact on state estimation accuracy. In *2007 IEEE Lausanne Power Tech*, pages 701–706, 2007. doi: 10.1109/PCT.2007.4538401.

[3] J. A. Boudreaux. Design, simulation, and construction of an ieee 14-bus power system. *LSU Master's Theses*, 9 2018. doi: 10.31390/gradschool_theses.4801.

[4] R. E. Caflisch. *Monte Carlo and quasi-monte Carlo Methods*. Dept. of Mathematics, University of California, Los Angeles, 1997.

[5] J. Cano Rodríguez, M. R. R. Mojumdar, J. Norniella, and G. Orcajo. Phase shifting transformer model for direct approach power flow studies. *International Journal of Electrical Power Energy Systems*, 91:71–79, 10 2017. doi: 10.1016/j.ijepes.2017.03.007.

[6] G. D'Antona. Power system static-state estimation with uncertain network parameters as input data. *IEEE Transactions on Instrumentation and Measurement*, 65: 1–10, 11 2016. doi: 10.1109/TIM.2016.2595999.

[7] J. J. Grainger. *Power system analysis*. McGraw-Hill, 1994.

[8] G. Krumpholz, K. Clements, and P. Davis. Power system observability: A practical algorithm using network topology. *IEEE Transactions on Power Apparatus and Systems*, PAS-99(4):1534–1542, 1980. doi: 10.1109/tpas.1980.319578.

[9] W.-H. Liu, F. Wu, and S.-M. Lun. Estimation of parameter errors from measurement residuals in state estimation (power systems). *IEEE Transactions on Power Systems*, 7(1):81–89, 1992. doi: 10.1109/59.141690.

[10] J. London, S. A. R. Piereti, R. A. S. Benedito, and N. G. Bretas. Redundancy and

observability analysis of conventional and pmu measurements. *IEEE Transactions on Power Systems*, 24(3):1629–1630, 2009. doi: 10.1109/TPWRS.2009.2021195.

[11] A. Monticelli. *State estimation in Electric Power Systems*, 1999. doi: 10.1007/978-1-4615-4999-4.

[12] A. Monticelli and F. F. Wu. Network observability: Identification of observable islands and measurement placement. *IEEE Power Engineering Review*, PER-5(5): 32–32, 1985. doi: 10.1109/mper.1985.5526567.

[13] M. H. Rajnish Kumar, Michael Giesselmann. State and parameter estimation of power systems using phasor measurement units as bilinear system model. *International Journal of Renewable Energy Research-IJRER*, 6(4), 2016.

[14] C. Rakpenthai, S. Premrudeepreechacharn, S. Uatrongjit, and N. Watson. Measurement placement for power system state estimation by decomposition technique. In *2004 11th International Conference on Harmonics and Quality of Power (IEEE Cat. No.04EX951)*, pages 414–418, 2004. doi: 10.1109/ICHQP.2004.1409391.

[15] C. Rich. 14 bus power flow test case. URL `http://labs.ece.uw.edu/pstca/pf14/pg_tca14bus.htm`.

[16] F. Schweppe and E. Handschin. Static state estimation in electric power systems. *Proceedings of the IEEE*, 62(7):972–982, 1974. doi: 10.1109/PROC.1974.9549.

[17] T. A. Stuart and C. J. Herczet. A sensitivity analysis of weighted least squares state estimation for power systems. *IEEE Transactions on Power Apparatus and Systems*, PAS-92(5):1696–1701, 1973. doi: 10.1109/TPAS.1973.293718.

[18] M. Wydra, P. Kacejko, and P. Gastolek. The impact of the power line conductors temperature on the optimal solution of generation distribution in the power system. In *2018 15th International Conference on the European Energy Market (EEM)*, pages 1–5, 2018. doi: 10.1109/EEM.2018.8469964.

[19] P. Zarco and A. Exposito. Power system parameter estimation: a survey. *IEEE Transactions on Power Systems*, 15(1):216–222, 2000. doi: 10.1109/59.852124.

[20] J. Zhao, J. Qi, Z. Huang, A. P. Meliopoulos, A. Gomez-Exposito, M. Netto, L. Mili, A. Abur, V. Terzija, I. Kamwa, and et al. Power system dynamic state estimation: Motivations, definitions, methodologies, and future work. *IEEE Transactions on Power Systems*, 34(4):3188–3198, 2019. doi: 10.1109/tpwrs.2019.2894769.

[21] J. Zhu and A. Abur. Effect of phasor measurements on the choice of reference bus for

state estimation. In *2007 IEEE Power Engineering Society General Meeting*, pages 1–5, 2007. doi: 10.1109/PES.2007.386175.

A | Appendix A State Variable Jacobian

This appendix deals with how to compute the Jacobian matrix H_1 concerning state variables for each type of measurement.

$$H_1 = \begin{bmatrix} \frac{\partial f_1}{\partial x_1} & \dots & \frac{\partial f_1}{\partial x_n} & \frac{\partial f_1}{\partial \theta_1} & \dots & \frac{\partial f_1}{\partial \theta_{n-1}} \\ \dots & & & & & \dots \\ \frac{\partial f_m}{\partial x_1} & \dots & & & & \frac{\partial f_m}{\partial \theta_{n-1}} \end{bmatrix}_{\tilde{x}_k, \tilde{\pi}} \tag{A.1}$$

A.1. Voltage Magnitude

Measurement A_1 shows the voltage magnitude squared:

$$A_{1,k} = \left|\overline{V_k}\right|^2 = \overline{V_k V_k}^* = x_k e^{j\theta_k} * x_k e^{-j\theta_k} = x_k^2 \tag{A.2}$$

Corresponding derivatives concerning state variables x, θ are:

$$\begin{aligned} \frac{\partial A_{1,k}}{\partial x_k} &= 2x_k \\ \\ \frac{\partial A_{1,k}}{\partial \theta_k} &= 0 \end{aligned} \tag{A.3}$$

A.2. Current Flow

Measurement A_2 shows the magnitude squared of current flow in-line:

$$A_2 = \left|\overline{I_{\mathrm{ij}}}\right|^2 = \overline{I_{\mathrm{ij}} I_{\mathrm{ij}}}^* \tag{A.4}$$

Where the current flow in-line $\overline{I_{\mathrm{ij}}}$ would be:

$$\overline{I_{\mathrm{ij}}} = \frac{\overline{V_{\mathrm{i}}} - \overline{V_{\mathrm{j}}}}{R + jX} + jB\overline{V_{\mathrm{i}}} = \frac{x_{\mathrm{i}} e^{j\theta_{\mathrm{i}}} - x_{\mathrm{j}} e^{j\theta_{\mathrm{j}}}}{R + jX} + jBx_{\mathrm{i}} e^{j\theta_{\mathrm{i}}} \tag{A.5}$$

Corresponding derivatives concerning state variables x, θ are:

$$\begin{aligned}
\frac{\partial A_{2,ij}}{\partial x_i} =& \left(\frac{e^{-i\theta_i}}{R - iX} - iBe^{-i\theta_i}\right)\left(iBx_i e^{i\theta_i} + \frac{x_i e^{i\theta_i} - x_j e^{i\theta_j}}{R + iX}\right) \\
&+ \left(iBe^{i\theta_i} + \frac{e^{i\theta_i}}{R + iX}\right)\left(\frac{x_i e^{-i\theta_i} - x_j e^{-i\theta_j}}{R - iX} - iBx_i e^{-i\theta_i}\right) \\
\frac{\partial A_{2,ij}}{\partial x_j} =& -\frac{e^{-i\theta_j}\left(iBx_i e^{i\theta_i} + \frac{x_i e^{i\theta_i} - x_j e^{i\theta_j}}{R+iX}\right)}{R - iX} \\
&- \frac{e^{i\theta_j}\left(\frac{x_i e^{-i\theta_i} - x_j e^{-i\theta_j}}{R-iX} - iBx_i e^{-i\theta_i}\right)}{R + iX} \\
\frac{\partial A_{2,ij}}{\partial \theta_i} =& \left(\frac{ix_i e^{i\theta_i}}{R + iX} - Bx_i e^{i\theta_i}\right)\left(\frac{x_i e^{-i\theta_i} - x_j e^{-i\theta_j}}{R - iX} - iBx_i e^{-i\theta_i}\right) \\
&+ \left(-Bx_i e^{-i\theta_i} - \frac{ix_i e^{-i\theta_i}}{R - iX}\right)\left(iBx_i e^{i\theta_i} + \frac{x_i e^{i\theta_i} - x_j e^{i\theta_j}}{R + iX}\right) \\
\frac{\partial A_{2,ij}}{\partial \theta_j} =& \frac{ix_j e^{-i\theta_j}\left(iBx_i e^{i\theta_i} + \frac{x_i e^{i\theta_i} - x_j e^{i\theta_j}}{R+iX}\right)}{R - iX} \\
&- \frac{ix_j e^{i\theta_j}\left(\frac{x_i e^{-i\theta_i} - x_j e^{-i\theta_j}}{R-iX} - iBx_i e^{-i\theta_i}\right)}{R + iX}
\end{aligned} \tag{A.6}$$

A.3. Injected Current

Measurement A_3 shows the magnitude squared of current injected on buses:

$$\begin{aligned} A_{3,k} &= \left| \sum_{m=1}^{n} \overline{I_{\mathrm{km}}} \right|^2 = \sum_{m=1} \overline{I_{\mathrm{km}}} \sum_{m=1} \overline{I_{\mathrm{km}}}^* \\ &= \sum_{n=1} \sum_{m=1} \overline{I_{\mathrm{kn}} I_{\mathrm{km}}}^* \end{aligned} \tag{A.7}$$

Corresponding derivatives concerning state variables x, θ are:

$$\begin{aligned} \frac{\partial A_{3,k}}{\partial x_i, \theta_i} &= \sum_{n=1} \sum_{m=1} \frac{\partial \overline{I_{\mathrm{kn}} I_{\mathrm{km}}}^*}{\partial x_i, \theta_i} \\ &= \sum_{n=1} \sum_{m=1} \frac{\partial \overline{I_{\mathrm{kn}}}}{\partial x_i, \theta_i} \overline{I_{\mathrm{km}}}^* + \sum_{n=1} \sum_{m=1} \frac{\partial \overline{I_{\mathrm{km}}}^*}{\partial x_i, \theta_i} \overline{I_{\mathrm{kn}}} \end{aligned} \tag{A.8}$$

In which $\frac{\partial \overline{I}}{\partial x_i, \theta_i}, \overline{I}^*, \frac{\partial \overline{I}^*}{\partial x_i, \theta_i}, \overline{I}$ can then be separately computed.

The current and conjugated current are:

$$\overline{I_{\mathrm{ij}}} = iBx_i e^{i\theta_i} + \frac{x_i e^{i\theta_i} - x_n e^{i\theta_j}}{R + iX} \tag{A.9}$$

$$\overline{I_{\mathrm{ij}}}^* = -iBx_i e^{-i\theta_i} + \frac{x_i e^{-i\theta_i} - x_m e^{-i\theta_j}}{R - iX} \tag{A.10}$$

And the partial derivatives with respect to state variables x, θ are:

$$\begin{aligned}
\frac{\partial \overline{I_{\mathrm{ij}}}}{\partial x_i} =& iBe^{i\theta_i} + \frac{e^{i\theta_i}}{R + iX} \\
\frac{\partial \overline{I_{\mathrm{ij}}}}{\partial x_j} =& -\frac{e^{i\theta_j}}{R + iX} \\
\frac{\partial \overline{I_{\mathrm{ij}}}}{\partial \theta_i} =& \frac{ix_i e^{i\theta_i}}{R + iX} - Bx_i e^{i\theta_i} \\
\frac{\partial \overline{I_{\mathrm{ij}}}}{\partial \theta_j} =& -\frac{ix_j e^{i\theta_j}}{R + iX} \\
\frac{\partial \overline{I_{\mathrm{ij}}}^*}{\partial x_i} =& \frac{e^{-i\theta_i}}{R - iX} - iBe^{-i\theta_i} \\
\frac{\partial \overline{I_{\mathrm{ij}}}^*}{\partial x_j} =& -\frac{e^{-i\theta_j}}{R - iX} \\
\frac{\partial \overline{I_{\mathrm{ij}}}^*}{\partial \theta_i} =& -Bx_i e^{-i\theta_i} - \frac{ix_i e^{-i\theta_i}}{R - iX} \\
\frac{\partial \overline{I_{\mathrm{ij}}}^*}{\partial \theta_j} =& \frac{ix_j e^{-i\theta_j}}{R - iX}
\end{aligned} \tag{A.11}$$

A.4. Active Power Flow

Measurement A_4 shows the active power flow in-line:

$$\begin{aligned} A_{4,ij} &= P_{\mathrm{ij}} = \mathrm{Real}(\overline{S_{\mathrm{ij}}}) = \mathrm{Real}(\overline{V_{\mathrm{i}} I_{\mathrm{ij}}^{*}}) \\ &= \frac{R x_i^2 \sin^2(\theta_i)}{R^2+X^2} + \frac{R x_i^2 \cos^2(\theta_i)}{R^2+X^2} - \frac{R x_i x_j \sin(\theta_i)\sin(\theta_j)}{R^2+X^2} \\ &- \frac{R x_i x_j \cos(\theta_i)\cos(\theta_j)}{R^2+X^2} - \frac{X x_i x_j \cos(\theta_i)\sin(\theta_j)}{R^2+X^2} + \frac{X x_i x_j \sin(\theta_i)\cos(\theta_j)}{R^2+X^2} \end{aligned} \tag{A.12}$$

Corresponding derivatives concerning state variables x, θ are:

$$\begin{aligned} \frac{\partial A_{4,ij}}{\partial x_i} =& \frac{2R x_i \sin^2(\theta_i)}{R^2+X^2} + \frac{2R x_i \cos^2(\theta_i)}{R^2+X^2} - \frac{R x_j \sin(\theta_i)\sin(\theta_j)}{R^2+X^2} \\ &- \frac{R x_j \cos(\theta_i)\cos(\theta_j)}{R^2+X^2} - \frac{X x_j \cos(\theta_i)\sin(\theta_j)}{R^2+X^2} + \frac{X x_j \sin(\theta_i)\cos(\theta_j)}{R^2+X^2} \\ \frac{\partial A_{4,ij}}{\partial x_j} =& - \frac{R x_i \sin(\theta_i)\sin(\theta_j)}{R^2+X^2} - \frac{R x_i \cos(\theta_i)\cos(\theta_j)}{R^2+X^2} + \frac{X x_i \sin(\theta_i)\cos(\theta_j)}{R^2+X^2} \\ &- \frac{X x_i \cos(\theta_i)\sin(\theta_j)}{R^2+X^2} \\ \frac{\partial A_{4,ij}}{\partial \theta_i} =& \frac{X x_i x_j \sin(\theta_i)\sin(\theta_j)}{R^2+X^2} + \frac{X x_i x_j \cos(\theta_i)\cos(\theta_j)}{R^2+X^2} \\ &+ \frac{R x_i x_j \sin(\theta_i)\cos(\theta_j)}{R^2+X^2} - \frac{R x_i x_j \cos(\theta_i)\sin(\theta_j)}{R^2+X^2} \\ \frac{\partial A_{4,ij}}{\partial \theta_j} =& - \frac{X x_i x_j \sin(\theta_i)\sin(\theta_j)}{R^2+X^2} - \frac{X x_i x_j \cos(\theta_i)\cos(\theta_j)}{R^2+X^2} - \frac{R x_i x_j \sin(\theta_i)\cos(\theta_j)}{R^2+X^2} \\ &+ \frac{R x_i x_j \cos(\theta_i)\sin(\theta_j)}{R^2+X^2} \end{aligned} \tag{A.13}$$

A.5. Reactive Power Flow

Measurement A_5 shows the reactive power flow in-line:

$$\begin{aligned} A_{5,ij} &= Q_{\mathrm{ij}} = \mathrm{Imag}(\overline{S_{\mathrm{ij}}}) = \mathrm{Imag}(\overline{V_{\mathrm{i}} I_{\mathrm{ij}}^{*}}) \\ &= -Bx_i^2 \sin^2(\theta_i) - Bx_i^2 \cos^2(\theta_i) + \frac{Xx_i^2 \sin^2(\theta_i)}{R^2+X^2} + \frac{Xx_i^2 \cos^2(\theta_i)}{R^2+X^2} \\ &- \frac{Xx_i x_j \sin(\theta_i)\sin(\theta_j)}{R^2+X^2} - \frac{Xx_i x_j \cos(\theta_i)\cos(\theta_j)}{R^2+X^2} + \frac{Rx_i x_j \cos(\theta_i)\sin(\theta_j)}{R^2+X^2} \\ &- \frac{Rx_i x_j \sin(\theta_i)\cos(\theta_j)}{R^2+X^2} \end{aligned} \tag{A.14}$$

Corresponding derivatives concerning state variables x, θ are:

$$\begin{aligned} \frac{\partial A_{5,ij}}{\partial x_i} &= -2Bx_i \sin^2(\theta_i) - 2Bx_i \cos^2(\theta_i) + \frac{2Xx_i \sin^2(\theta_i)}{R^2+X^2} \\ &+ \frac{2Xx_i \cos^2(\theta_i)}{R^2+X^2} - \frac{Xx_j \sin(\theta_i)\sin(\theta_j)}{R^2+X^2} - \frac{Xx_j \cos(\theta_i)\cos(\theta_j)}{R^2+X^2} \\ &+ \frac{Rx_j \cos(\theta_i)\sin(\theta_j)}{R^2+X^2} - \frac{Rx_j \sin(\theta_i)\cos(\theta_j)}{R^2+X^2} \end{aligned}$$

$$\begin{aligned} \frac{\partial A_{5,ij}}{\partial x_j} &= -\frac{Xx_i \sin(\theta_i)\sin(\theta_j)}{R^2+X^2} - \frac{Xx_i \cos(\theta_i)\cos(\theta_j)}{R^2+X^2} - \frac{Rx_i \sin(\theta_i)\cos(\theta_j)}{R^2+X^2} \\ &\frac{Rx_i \cos(\theta_i)\sin(\theta_j)}{R^2+X^2} \end{aligned} \tag{A.15}$$

$$\begin{aligned} \frac{\partial A_{5,ij}}{\partial \theta_i} &= -\frac{Rx_i x_j \sin(\theta_i)\sin(\theta_j)}{R^2+X^2} - \frac{Rx_i x_j \cos(\theta_i)\cos(\theta_j)}{R^2+X^2} + \frac{Xx_i x_j \sin(\theta_i)\cos(\theta_j)}{R^2+X^2} \\ &- \frac{Xx_i x_j \cos(\theta_i)\sin(\theta_j)}{R^2+X^2} \end{aligned}$$

$$\begin{aligned} \frac{\partial A_{5,ij}}{\partial \theta_j} &= \frac{Rx_i x_j \sin(\theta_i)\sin(\theta_j)}{R^2+X^2} + \frac{Rx_i x_j \cos(\theta_i)\cos(\theta_j)}{R^2+X^2} - \frac{Xx_i x_j \sin(\theta_i)\cos(\theta_j)}{R^2+X^2} \\ &+ \frac{Xx_i x_j \cos(\theta_i)\sin(\theta_j)}{R^2+X^2} \end{aligned}$$

A.6. Active Injected Power

Measurement A_6 shows the active injected power:

$$A_{6,k} = P_k = \sum_{j=1}^{n} P_{\mathrm{kj}} = \sum_{j=1}^{n} A_{4,\mathrm{kj}} \tag{A.16}$$

Corresponding derivatives concerning state variables x, θ can be derived from the in-line power flow formulae:

$$\frac{\partial A_{6,k}}{\partial x_i, \theta_i} = \sum_{j=1}^{n} \frac{\partial A_{4,kj}}{\partial x_i, \theta_i} \tag{A.17}$$

A.7. Reactive Injected Power

Measurement A_7 shows the reactive injected power:

$$A_{7,k} = Q_k = \sum_{j=1}^{n} Q_{\mathrm{kj}} = \sum_{j=1}^{n} A_{5,\mathrm{kj}} \tag{A.18}$$

Corresponding derivatives concerning state variables x, θ can be derived from the in-line power flow formulae:

$$\frac{\partial A_{6,k}}{\partial x_i, \theta_i} = \sum_{j=1}^{n} \frac{\partial A_{6,kj}}{\partial x_i, \theta_i} \tag{A.19}$$

B | Appendix B parameter Jacobian

This appendix deals with how to compute the Jacobian matrix H_1 concerning parameter data for each type of measurement, for the use of GWLS and EWLS.

$$H_2 = \begin{bmatrix} \frac{\partial f_1}{\partial R_1} & \cdots & \frac{\partial f_1}{\partial R_n} & \frac{\partial f_1}{\partial X_1} & \cdots & \frac{\partial f_1}{\partial X_n} & \frac{\partial f_1}{\partial B_1} & \cdots & \frac{\partial f_1}{\partial B_n} \\ \cdots & & & & & & & & \\ \frac{\partial f_m}{\partial R_1} & & & & \cdots & & & & \frac{\partial f_m}{\partial B_n} \end{bmatrix} \tag{B.1}$$

B.1. Voltage Magnitude

Measurement A_1 shows the voltage magnitude squared:

$$A_{1,k} = \left|\overline{V_k}\right|^2 = \overline{V_k V_k}^* = x_k e^{j\theta_k} * x_k e^{-j\theta_k} = x_k^2 \tag{B.2}$$

Corresponding derivatives concerning parameter R, X, B are:

$$\begin{aligned} \frac{\partial A_{1,k}}{\partial R} &= 0 \\ \frac{\partial A_{1,k}}{\partial X} &= 0 \\ \frac{\partial A_{1,k}}{\partial B} &= 0 \end{aligned} \tag{B.3}$$

B.2. Current Flow

Measurement A_2 shows the magnitude squared of current flow in-line:

$$A_2 = \left|\overline{I_{\mathrm{ij}}}\right|^2 = \overline{I_{\mathrm{ij}} I_{\mathrm{ij}}}^* \tag{B.4}$$

Where the current flow in-line $\overline{I_{\mathrm{ij}}}$ would be:

$$\overline{I_{\mathrm{ij}}} = \frac{\overline{V_{\mathrm{i}}} - \overline{V_{\mathrm{j}}}}{R_{\mathrm{k}} + jX_{\mathrm{k}}} + jB_{\mathrm{k}}\overline{V_{\mathrm{i}}} = \frac{x_{\mathrm{i}}e^{j\theta_{\mathrm{i}}} - x_{\mathrm{j}}e^{j\theta_{\mathrm{j}}}}{R_{\mathrm{k}} + jX_{\mathrm{k}}} + jB_{\mathrm{k}}x_{\mathrm{i}}e^{j\theta_{\mathrm{i}}} \tag{B.5}$$

Corresponding derivatives concerning parameter R, X, B are:

$$\begin{aligned}
\frac{\partial A_{4,ij}}{\partial R} =& -\frac{\left(x_i e^{-i\theta_i} - x_j e^{-i\theta_j}\right)\left(iBx_i e^{i\theta_i} + \frac{x_i e^{i\theta_i} - x_j e^{i\theta_j}}{R+iX}\right)}{(R-iX)^2} \\
& -\frac{\left(x_i e^{i\theta_i} - x_j e^{i\theta_j}\right)\left(\frac{x_i e^{-i\theta_i} - x_j e^{-i\theta_j}}{R-iX} - iBx_i e^{-i\theta_i}\right)}{(R+iX)^2}
\end{aligned}$$

$$\begin{aligned}
\frac{\partial A_{4,ij}}{\partial X} =& \frac{i\left(x_i e^{-i\theta_i} - x_j e^{-i\theta_j}\right)\left(iBx_i e^{i\theta_i} + \frac{x_i e^{i\theta_i} - x_j e^{i\theta_j}}{R+iX}\right)}{(R-iX)^2} \\
& -\frac{i\left(x_i e^{i\theta_i} - x_j e^{i\theta_j}\right)\left(\frac{x_i e^{-i\theta_i} - x_j e^{-i\theta_j}}{R-iX} - iBx_i e^{-i\theta_i}\right)}{(R+iX)^2}
\end{aligned} \tag{B.6}$$

$$\begin{aligned}
\frac{\partial A_{4,ij}}{\partial B} =& ix_i e^{i\theta_i}\left(\frac{x_i e^{-i\theta_i} - x_j e^{-i\theta_j}}{R-iX} - iBx_i e^{-i\theta_i}\right) \\
& - ix_i e^{-i\theta_i}\left(iBx_i e^{i\theta_i} + \frac{x_i e^{i\theta_i} - x_j e^{i\theta_j}}{R+iX}\right)
\end{aligned}$$

B.3. Injected Current

Measurement A_3 shows the magnitude squared of current injected on buses:

$$\begin{aligned} A_{3,k} &= \left| \sum_{m=1}^{n} \overline{I_{\mathrm{km}}} \right|^2 = \sum_{m=1} \overline{I_{\mathrm{km}}} \sum_{m=1} \overline{I_{\mathrm{km}}}^* \\ &= \sum_{n=1} \sum_{m=1} \overline{I_{\mathrm{kn}} I_{\mathrm{km}}}^* \end{aligned} \tag{B.7}$$

Corresponding derivatives concerning parameter R, X, B are:

$$\begin{aligned} \frac{\partial A_{3,k}}{\partial x_i, \theta_i} &= \sum_{n=1} \sum_{m=1} \frac{\partial \overline{I_{\mathrm{kn}} I_{\mathrm{km}}}^*}{\partial x_i, \theta_i} \\ &= \sum_{n=1} \sum_{m=1} \frac{\partial \overline{I_{\mathrm{kn}}}}{\partial x_i, \theta_i} \overline{I_{\mathrm{km}}}^* + \sum_{n=1} \sum_{m=1} \frac{\partial \overline{I_{\mathrm{km}}}^*}{\partial x_i, \theta_i} \overline{I_{\mathrm{kn}}} \end{aligned} \tag{B.8}$$

In which $\frac{\partial \bar{I}}{\partial x_i, \theta_i}, \overline{I}^*, \frac{\partial \bar{I}^*}{\partial x_i, \theta_i}, \overline{I}$ can then be separately computed.

The current and conjugated current are:

$$\overline{I_{\mathrm{ij}}} = iBx_i e^{i\theta_i} + \frac{x_i e^{i\theta_i} - x_n e^{i\theta_j}}{R + iX} \tag{B.9}$$

$$\overline{I_{\mathrm{ij}}}^* = -iBx_i e^{-i\theta_i} + \frac{x_i e^{-i\theta_i} - x_m e^{-i\theta_j}}{R - iX} \tag{B.10}$$

And the partial derivatives with respect to parameter R, X, B, θ are:

$$\begin{aligned}
\frac{\partial \overline{I_{\mathrm{ij}}}}{\partial R} &= -\frac{x_i e^{i\theta_i} - x_j e^{i\theta_j}}{(R+iX)^2} \\
\frac{\partial \overline{I_{\mathrm{ij}}}}{\partial X} &= -\frac{i\left(x_i e^{i\theta_i} - x_j e^{i\theta_j}\right)}{(R+iX)^2} \\
\frac{\partial \overline{I_{\mathrm{ij}}}}{\partial B} &= i x_i e^{i\theta_i} \\
\frac{\partial \overline{I_{\mathrm{ij}}}^*}{\partial R} &= -\frac{x_i e^{-i\theta_i} - x_j e^{-i\theta_j}}{(R-iX)^2} \\
\frac{\partial \overline{I_{\mathrm{ij}}}^*}{\partial X} &= \frac{i\left(x_i e^{-i\theta_i} - x_j e^{-i\theta_j}\right)}{(R-iX)^2} \\
\frac{\partial \overline{I_{\mathrm{ij}}}^*}{\partial B} &= \frac{x_i e^{-i\theta_i} - x_j e^{-i\theta_j}}{R-iX} - iBx_i e^{-i\theta_i}
\end{aligned} \tag{B.11}$$

B.4. Active Power Flow

Measurement A_4 shows the active power flow in-line:

$$\begin{aligned} A_{4,ij} &= P_{\mathrm{ij}} = \mathrm{Real}(\overline{S_{\mathrm{ij}}}) = \mathrm{Real}(\overline{V_{\mathrm{i}} I_{\mathrm{ij}}^{*}}) \\ &= \frac{R x_i^2 \sin^2(\theta_i)}{R^2+X^2} + \frac{R x_i^2 \cos^2(\theta_i)}{R^2+X^2} - \frac{R x_i x_j \sin(\theta_i)\sin(\theta_j)}{R^2+X^2} \\ &- \frac{R x_i x_j \cos(\theta_i)\cos(\theta_j)}{R^2+X^2} - \frac{X x_i x_j \cos(\theta_i)\sin(\theta_j)}{R^2+X^2} + \frac{X x_i x_j \sin(\theta_i)\cos(\theta_j)}{R^2+X^2} \end{aligned} \tag{B.12}$$

Corresponding derivatives concerning parameter R, X, B are:

$$\begin{aligned} \frac{\partial A_4}{\partial R} =& -\frac{2R^2 x_i^2 \sin^2(\theta_i)}{(R^2+X^2)^2} + \frac{x_i^2 \sin^2(\theta_i)}{R^2+X^2} - \frac{2R^2 x_i^2 \cos^2(\theta_i)}{(R^2+X^2)^2} \\ &+ \frac{x_i^2 \cos^2(\theta_i)}{R^2+X^2} + \frac{2R^2 x_i x_j \sin(\theta_i)\sin(\theta_j)}{(R^2+X^2)^2} - \frac{x_i x_j \sin(\theta_i)\sin(\theta_j)}{R^2+X^2} \\ &+ \frac{2R^2 x_i x_j \cos(\theta_i)\cos(\theta_j)}{(R^2+X^2)^2} - \frac{x_i x_j \cos(\theta_i)\cos(\theta_j)}{R^2+X^2} \\ &+ \frac{2RX x_i x_j \cos(\theta_i)\sin(\theta_j)}{(R^2+X^2)^2} - \frac{2RX x_i x_j \sin(\theta_i)\cos(\theta_j)}{(R^2+X^2)^2} \end{aligned}$$

$$\begin{aligned} \frac{\partial A_4}{\partial X} =& -\frac{2RX x_i^2 \sin^2(\theta_i)}{(R^2+X^2)^2} - \frac{2RX x_i^2 \cos^2(\theta_i)}{(R^2+X^2)^2} + \frac{2RX x_i x_j \sin(\theta_i)\sin(\theta_j)}{(R^2+X^2)^2} \\ &+ \frac{2RX x_i x_j \cos(\theta_i)\cos(\theta_j)}{(R^2+X^2)^2} + \frac{2X^2 x_i x_j \cos(\theta_i)\sin(\theta_j)}{(R^2+X^2)^2} \\ &- \frac{2X^2 x_i x_j \sin(\theta_i)\cos(\theta_j)}{(R^2+X^2)^2} + \frac{x_i x_j \sin(\theta_i)\cos(\theta_j)}{R^2+X^2} \\ &- \frac{x_i x_j \cos(\theta_i)\sin(\theta_j)}{R^2+X^2} \end{aligned} \tag{B.13}$$

$$\frac{\partial A_4}{\partial B} = 0$$

B.5. Reactive Power Flow

Measurement A_5 shows the reactive power flow in-line:

$$\begin{aligned} A_{5,ij} &= Q_{\mathrm{ij}} = \mathrm{Imag}(\overline{S_{\mathrm{ij}}}) = \mathrm{Imag}(\overline{V_{\mathrm{i}} I_{\mathrm{ij}}^{*}}) \\ &= -Bx_i^2 \sin^2(\theta_i) - Bx_i^2 \cos^2(\theta_i) + \frac{Xx_i^2 \sin^2(\theta_i)}{R^2+X^2} + \frac{Xx_i^2 \cos^2(\theta_i)}{R^2+X^2} \\ &- \frac{Xx_ix_j \sin(\theta_i)\sin(\theta_j)}{R^2+X^2} - \frac{Xx_ix_j \cos(\theta_i)\cos(\theta_j)}{R^2+X^2} + \frac{Rx_ix_j \cos(\theta_i)\sin(\theta_j)}{R^2+X^2} \\ &- \frac{Rx_ix_j \sin(\theta_i)\cos(\theta_j)}{R^2+X^2} \end{aligned} \tag{B.14}$$

Corresponding derivatives concerning parameter R, X, B are:

$$\begin{aligned} \frac{\partial A_5}{\partial R} =& - \frac{2RXx_i^2 \sin^2(\theta_i)}{\left(R^2+X^2\right)^2} - \frac{2RXx_i^2 \cos^2(\theta_i)}{\left(R^2+X^2\right)^2} + \frac{2RXx_ix_j \sin(\theta_i)\sin(\theta_j)}{\left(R^2+X^2\right)^2} \\ &+ \frac{2RXx_ix_j \cos(\theta_i)\cos(\theta_j)}{\left(R^2+X^2\right)^2} + \frac{2R^2x_ix_j \sin(\theta_i)\cos(\theta_j)}{\left(R^2+X^2\right)^2} \\ &- \frac{2R^2x_ix_j \cos(\theta_i)\sin(\theta_j)}{\left(R^2+X^2\right)^2} + \frac{x_ix_j \cos(\theta_i)\sin(\theta_j)}{R^2+X^2} \\ &- \frac{x_ix_j \sin(\theta_i)\cos(\theta_j)}{R^2+X^2} \end{aligned}$$

$$\begin{aligned} \frac{\partial A_5}{\partial X} =& - \frac{2X^2x_i^2 \sin^2(\theta_i)}{\left(R^2+X^2\right)^2} + \frac{x_i^2 \sin^2(\theta_i)}{R^2+X^2} - \frac{2X^2x_i^2 \cos^2(\theta_i)}{\left(R^2+X^2\right)^2} \\ &+ \frac{x_i^2 \cos^2(\theta_i)}{R^2+X^2} + \frac{2X^2x_ix_j \sin(\theta_i)\sin(\theta_j)}{\left(R^2+X^2\right)^2} - \frac{x_ix_j \sin(\theta_i)\sin(\theta_j)}{R^2+X^2} \\ &+ \frac{2X^2x_ix_j \cos(\theta_i)\cos(\theta_j)}{\left(R^2+X^2\right)^2} - \frac{x_ix_j \cos(\theta_i)\cos(\theta_j)}{R^2+X^2} \\ &+ \frac{2RXx_ix_j \sin(\theta_i)\cos(\theta_j)}{\left(R^2+X^2\right)^2} - \frac{2RXx_ix_j \cos(\theta_i)\sin(\theta_j)}{\left(R^2+X^2\right)^2} \end{aligned} \tag{B.15}$$

$$\frac{\partial A_5}{\partial B} = - x_i^2 \sin^2(\theta_i) - x_i^2 \cos^2(\theta_i)$$

B.6. Active Injected Power

Measurement A_6 shows the active injected power:

$$A_{6,k} = P_k = \sum_{j=1}^{n} P_{\mathrm{kj}} = \sum_{j=1}^{n} A_{4,\mathrm{kj}} \tag{B.16}$$

Corresponding derivatives concerning parameter R, X, B can be derived from the in-line power flow formulae:

$$\frac{\partial A_{6,k}}{\partial x_i, \theta_i} = \sum_{j=1}^{n} \frac{\partial A_{4,kj}}{\partial x_i, \theta_i} \tag{B.17}$$

B.7. Reactive Injected Power

Measurement A_7 shows the reactive injected power:

$$A_{7,k} = Q_k = \sum_{j=1}^{n} Q_{\mathrm{kj}} = \sum_{j=1}^{n} A_{5,\mathrm{kj}} \tag{B.18}$$

Corresponding derivatives concerning parameter R, X, B can be derived from the in-line power flow formulae:

$$\frac{\partial A_{6,k}}{\partial x_i, \theta_i} = \sum_{j=1}^{n} \frac{\partial A_{6,kj}}{\partial x_i, \theta_i} \tag{B.19}$$

C | Appendix C IEEE14 Bus System

IEEE14 bus system is a simple representation of a portion of the American power grid in 1962. This classical test system has 5 generators, 11 loads and as its name indicates, 14 buses.[15]

It declares its base values as follows:

- Base power = 10 kVA
- Base Voltage = 230 V

All units of data given in the following are in p.u. unless otherwise specified.

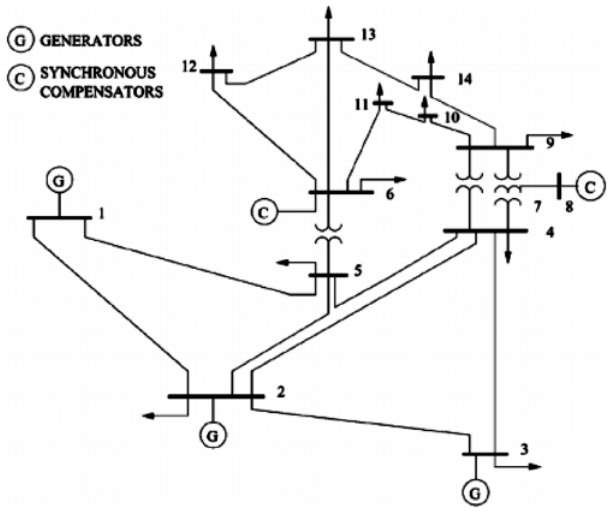

Figure C.1: IEEE14 Bus System [15]

The system consists of 20 lines, with their parameter data (line resistance, line reactance, half-line charging susceptance) shown in table C.1:

Line Numb.	From Bus	To Bus	Line Res.	Line Rea.	Half Sus.
1	1	2	0.01938	0.05917	0.0264
2	1	5	0.05403	0.22304	0.0246
3	2	3	0.04699	0.19797	0.0219
4	2	4	0.05811	0.17632	0.017
5	2	5	0.05695	0.17388	0.0173
6	3	4	0.06701	0.17103	0.0064
7	4	5	0.01335	0.04211	0
8	4	7	0	0.20912	0
9	4	9	0	0.55618	0
10	5	6	0	0.25202	0
11	6	11	0.09498	0.1989	0
12	6	12	0.12291	0.25581	0
13	6	13	0.06615	0.13027	0
14	7	8	0	0.17615	0
15	7	9	0	0.11001	0
16	9	10	0.03181	0.0845	0
17	9	14	0.12711	0.27038	0
18	10	11	0.08205	0.19207	0
19	12	13	0.22092	0.19988	0
20	13	14	0.17093	0.34802	0

Table C.1: IEEE14 Bus System Parameter Data

Tap-changing transformer data are shown in C.2:

Tap Numb.	From Bus	To Bus	Tap Set.
1	4	7	0.978
2	4	9	0.969
3	5	6	0.932

Table C.2: IEEE14 Bus System Tap-changing Transformer Data

Shunt capacitors data are shown in C.3

Bus Numb.	Sus.
9	0.19

Table C.3: IEEE14 Bus System Shunt Capacitor Data

Bus data concerning generators, loads are shown in C.4:

Bus Numb.	**Mag.**	**Pha.**	**Gen. Real**	**Gen. Reac.**	**Load Real**	**Load Reac.**	Q_min **(Mvar)**	Q_max **(Mvar)**
1	1.06	0	114.17	-16.9	0	0	0	10
2	1.045	0	40	0	21.7	12.7	-42	50
3	1.01	0	0	0	94.2	19.1	23.4	40
4	1	0	0	0	47.8	-3.9	-	-
5	1	0	0	0	7.6	1.6	-	-
6	1	0	0	0	11.2	7.5	-	-
7	1	0	0	0	0	0	-	-
8	1	0	0	0	0	0	-	-
9	1	0	0	0	29.5	16.6	-	-
10	1	0	0	0	9	5.8	-	-
11	1	0	0	0	3.5	1.8	-	-
12	1	0	0	0	6.1	1.6	-	-
13	1	0	0	0	13.8	5.8	-	-
14	1	0	0	0	14.9	5	-	-

Table C.4: IEEE14 Bus System Data

List of Figures

List of Tables

List of Symbols

Variable	Description
$\tilde{x}$	state variable vector
y	measurement data
π	parameter data
d	data (containing both listed above)
R	line resistance
X	line reactance
B	half-line charging susceptance
x	bus voltage magnitude
θ	bus voltage phasor
δx	errors of variable x
x_t	indicates the true value of variable x
Σ_x	variance-covariance matrix of variable x

Acknowledgements

I would like to express my deepest gratitude to my supervisor Prof. Gabriele D'antona. His guidance has been a tremendous help on every aspect of this work.